The Plant Cell, Vol. 30: 1710–1728, August 2018, www.plantcell.org © 2018 ASPB.

The Interaction between DELLA and ARF/IAA Mediates Crosstalk between Gibberellin and Auxin Signaling to Control Fruit Initiation in Tomato

Jianhong Hu,[a] Alon Israeli,[b] Naomi Ori,[b] and Tai-ping Sun[a,1]

[a]Department of Biology, Duke University, Durham, North Carolina 27708
[b]The Robert H. Smith Institute of Plant Sciences and Genetics in Agriculture, Hebrew University, Rehovot 76100, Israel

ORCID IDs: 0000-0003-3927-9240 (J.H.); 0000-0002-3339-2042 (A.I.); 0000-0002-5129-5369 (N.O.); 0000-0001-5223-2936 (T.-p.S.)

Fruit initiation following fertilization in angiosperms is strictly regulated by phytohormones. In tomato (*Solanum lycopersicum*), auxin and gibberellin (GA) play central roles in promoting fruit initiation. Without fertilization, elevated GA or auxin signaling can induce parthenocarpy (seedless fruit production). The GA-signaling repressor SlDELLA and auxin-signaling components SlIAA9 and SlARF7 repress parthenocarpy, but the underlying mechanism is unknown. Here, we show that SlDELLA and the SlARF7/SlIAA9 complex mediate crosstalk between GA and auxin pathways to regulate fruit initiation. Yeast-two-hybrid and coimmunoprecipitation assays showed that SlARF7 and additional activator SlARFs interact with SlDELLA and SlIAA9 through distinct domains. SlARF7/SlIAA9 and SlDELLA antagonistically modulate the expression of feedback-regulated genes involved in GA and auxin metabolism, whereas SlARF7/SlIAA9 and SlDELLA coregulate the expression of fruit growth-related genes. Analysis of *procera* (*della*), *SlARF7 RNAi* (with downregulated expression of multiple activator *SlARFs*), and *entire* (*iaa9*) single and double mutants indicated that these genes additively affect parthenocarpy, supporting the notion that the SlARFs/SlIAA9 and SlDELLA interaction plays an important role in regulating fruit initiation. Analysis of the GA-deficient mutant *gib1* showed that active GA biosynthesis and signaling are required for auxin-induced fruit initiation. Our study reveals how direct crosstalk between auxin- and GA-signaling components is critical for tomato fruit initiation.

Fruit development is an important reproductive process in angiosperms (Gillaspy et al., 1993). Fruits are derived from ovaries, whose default fate is senescence. Only upon successful pollination and fertilization can an ovary develop into a fruit; this process is called fruit initiation or fruit set. In general, fruit development starts with extensive cell division, followed by cell expansion to provide a suitable environment for maturation of the developing seeds inside the fruit (Gillaspy et al., 1993; Ruan et al., 2012). Plant hormones play pivotal roles in fruit development. In particular, auxin and gibberellin (GA) are the major hormones that promote fruit initiation and subsequent growth to enable full-size fruit production (Srivastava and Handa, 2005; Ruan et al., 2012; Seymour et al., 2013). The current model suggests that both auxin and GA are produced in young seeds immediately after fertilization to promote the fruit initiation process. Importantly, the application of either hormone can trigger parthenocarpy (formation of seedless fruit from an unpollinated ovary) in the absence of fertilization, indicating that the activation of auxin or GA signaling is required for fruit initiation (Gorguet et al., 2005). Parthenocarpy is a desirable agronomic trait that uncouples fruit development from the requirement for fertilization, creating seedless fruits that are often preferred by consumers. Auxin and GA are also involved in postfertilization fruit growth, with distinct functions; in general, auxin promotes cell division and GA functions in later cell expansion (Serrani et al., 2007).

In recent years, the molecular mechanisms of the early auxin and GA signaling cascades have been well characterized, particularly in *Arabidopsis thaliana* and rice (*Oryza sativa*); these mechanisms are conserved in angiosperms. Auxin activates its signaling pathway by binding to its nucleus-localized receptors TIR1/AFBs, which are F-box proteins (subunits of an SCF ubiquitin E3 ligase) that recruit downstream repressors AUX/IAA (IAA) proteins for polyubiquitination and subsequent degradation by the 26S proteasome (Dharmasiri et al., 2005; Kepinski and Leyser, 2005; Mockaitis and Estelle, 2008; Salehin et al., 2015). In the absence of auxin, IAA proteins bind to AUXIN RESPONSE FACTOR (ARF) transcription factors to repress auxin signaling. When auxin levels are elevated, auxin induces the rapid degradation of IAA proteins, allowing ARF monomers and/or dimers to activate auxin-responsive genes (Guilfoyle and Hagen, 2007; Guilfoyle, 2015; Salehin et al., 2015). Both IAAs and ARFs belong to large gene families, adding more layers of regulation and complexity to auxin signaling. Several members of the IAA and ARF families have been shown to function in fruit development. In tomato (*Solanum lycopersicum*), a model plant for fleshy fruit development, the *SlIAA9* loss-of-function mutant *entire* (Zhang et al., 2007) and antisense lines (Wang et al., 2005) showed strong parthenocarpy, indicating its function as a repressor of tomato fruit set. Downregulation of *SlARF7* by RNAi also confers parthenocarpy (de Jong et al., 2009). In addition, a loss-of-function mutation in Arabidopsis *ARF8* results in a parthenocarpic-fruit

[1]Address correspondence to tps@duke.edu.
The author responsible for distribution of materials integral to the findings presented in this article in accordance with the policy described in the Instructions for Authors (www.plantcell.org) is: Tai-ping Sun (tps@duke.edu).
www.plantcell.org/cgi/doi/10.1105/tpc.18.00363

phenotype (Goetz et al., 2006). Similarly, downregulation of the eggplant *ARF8* (*SmARF8*) by RNAi causes parthenocarpy (Du et al., 2016). Interestingly, overexpression of *SmARF8* in Arabidopsis also promotes parthenocarpy (Du et al., 2016). These reports suggest that auxin-signaling components interact to regulate fruit set. Similar to auxin signaling, the GA response pathway is negatively regulated by its central repressors DELLA proteins, which are nucleus-localized transcriptional regulators (Peng et al., 1997; Silverstone et al., 1998; Sun, 2010; Davière and Achard, 2016). Binding of bioactive GA to its nuclear receptor GIBBERELLIN INSENSITIVE DWARF1 (GID1) enhances the GID1-DELLA interaction, resulting in rapid degradation of DELLAs via the ubiquitin-proteasome pathway, thus releasing growth repression imposed by DELLAs (McGinnis et al., 2003; Ueguchi-Tanaka et al., 2005; Murase et al., 2008). Arabidopsis contains five *DELLA* genes: the quadruple mutant (with functional *RGL3* and no other functional *DELLA* genes) and the quintuple *della* (*global*) mutant show equally strong parthenocarpy, indicating that *RGA*, *GA INSENSITIVE*, *RGL1*, and *RGL2* play major roles in this process (Dorcey et al., 2009; Fuentes et al., 2012). Similarly, in tomato, mutations and RNAi downregulation of the only *SlDELLA* gene (*PROCERA*) cause parthenocarpy (Martí et al., 2007; Carrera et al., 2012; Livne et al., 2015), confirming that PROCERA is a repressor of fruit initiation.

The elucidation of auxin and GA signaling cascades has greatly facilitated investigations of how these hormones coordinate with each other to regulate fruit development. The current model (based on studies in several organisms) suggests that auxin acts upstream of GA during fruit development (Serrani et al., 2008; Dorcey et al., 2009; Ozga et al., 2009). In Arabidopsis, the fertilization-induced auxin response or auxin application triggers GA biosynthesis, whereas GA application does not induce the auxin response (Dorcey et al., 2009). In addition, auxin treatment of the *della global* mutant does not further stimulate its parthenocarpy, implying that in Arabidopsis, auxin-induced parthenocarpy occurs entirely through DELLA-dependent GA signaling (Fuentes et al., 2012). In tomato, parthenocarpic induction by auxin is also mediated at least partially by GA, as cotreatment with paclobutrazol (PAC; an inhibitor of GA biosynthesis) and auxin greatly reduces parthenocarpy, which can be reversed by coapplication with GA (Serrani et al., 2008). In addition, bioactive GA levels are elevated in auxin (treatment or *iaa9*/*entire*)-induced parthenocarpic fruits due to increased expression of GA biosynthesis genes and reduced expression of GA catabolism genes (Serrani et al., 2008; Mignolli et al., 2015). Therefore, it was suggested that auxin induces fruit initiation in part through the induction of GA biosynthesis. Auxin and GA are thought to play distinct roles in postinitiation fruit growth, because auxin- and GA-induced parthenocarpic fruits have different morphologies (Serrani et al., 2007). Auxin increases fruit size by increasing the number of pericarp cell layers and enlarging the placenta. GA treatment only induces the formation of medium-size fruit with larger cells but fewer cell layers. Simultaneous application of both hormones can promote parthenocarpy, yielding fruit with a size and cellular structure similar to those of pollinated fruit. Overall, these studies point to a possible mechanism in which auxin acts upstream of GA during fruit initiation, while these two hormones might play diverse roles during fruit growth.

In addition to the current model of auxin acting upstream of GA, evidence suggesting direct crosstalk between auxin and GA signaling pathways has emerged in recent years. RGA (a major Arabidopsis DELLA) was recently shown to interact with three activator ARFs (AtARF6, AtARF7, and AtARF8) by yeast two-hybrid (Y2H) assays and coimmunoprecipitation (co-IP) (Oh et al., 2014). Through this interaction, RGA appears to inhibit the binding of AtARF6 to the promoters of its target genes that function in hypocotyl elongation (Oh et al., 2014). However, the effect of the DELLA-ARF interaction in planta has not been confirmed by genetic analysis.

In this study, we report that GA and auxin regulate tomato fruit initiation through crosstalk between SlDELLA and SlARF7/SlIAA9. Y2H and co-IP assays revealed that SlARF7 and additional activator SlARFs bind to SlDELLA and SlIAA9 through distinct domains. RT-qPCR and transient expression analyses showed that the SlARF7/SlIAA9 complex and SlDELLA antagonistically regulate the expression of feedback-regulated genes involved in auxin and GA metabolism. By contrast, the SlARF7/SlIAA9 complex and SlDELLA additively coregulate the expression of downstream growth-related genes. To investigate the effect of the DELLA-ARF7/IAA9 interaction in planta, we generated double mutants using *procera*, *SlARF7 RNAi*, and *entire* (*iaa9*) mutants. Phenotype and expression analysis indicated that these mutations additively affect parthenocarpic fruit development. Moreover, auxin application and *ARF7 RNAi*/*iaa9* mutations failed to promote parthenocarpy in the GA-deficient *gib1* mutant, indicating that active GA biosynthesis and signaling are required for auxin-induced fruit initiation. Genetic analysis of *slarf7* and *slarf5* single and double mutants showed that the parthenocarpic phenotype of the *SlARF7 RNAi* line is caused by downregulation of multiple activator *SlARFs.* Overall, our study reveals a mechanism in which direct crosstalk between auxin and GA signaling controls tomato fruit initiation.

RESULTS

GA Signaling Repressor SlDELLA Interacts with Auxin Signaling Transcription Factor SlARFs

Previous studies have shown that both SlARF7 and SlDELLA affect tomato fruit initiation (Martí et al., 2007; de Jong et al., 2009). We hypothesized that SlARF7 and SlDELLA mediate crosstalk between GA and auxin signaling during fruit development. To test whether SlARF7 and SlDELLA directly interact, we performed a Y2H assay. A truncated SlDELLA construct (DELLA-CT3, encoding the C-terminal portion of SlDELLA from amino acid residues 166–588) was used as the bait because full-length SlDELLA alone can activate the reporter genes in Y2H assays. We found that SlDELLA indeed interacted with SlARF7 in this assay (Figure 1A). We then tested whether this interaction occurs in plant cells by co-IP using the transient expression system in wild tobacco (*Nicotiana benthamiana*). HA-SlDELLA was transiently expressed alone or coexpressed with Myc-SlARF7 or Myc-GUS-NLS (as a negative control). After IP using anti-Myc antibody-conjugated beads, HA-SlDELLA was coimmunoprecipitated

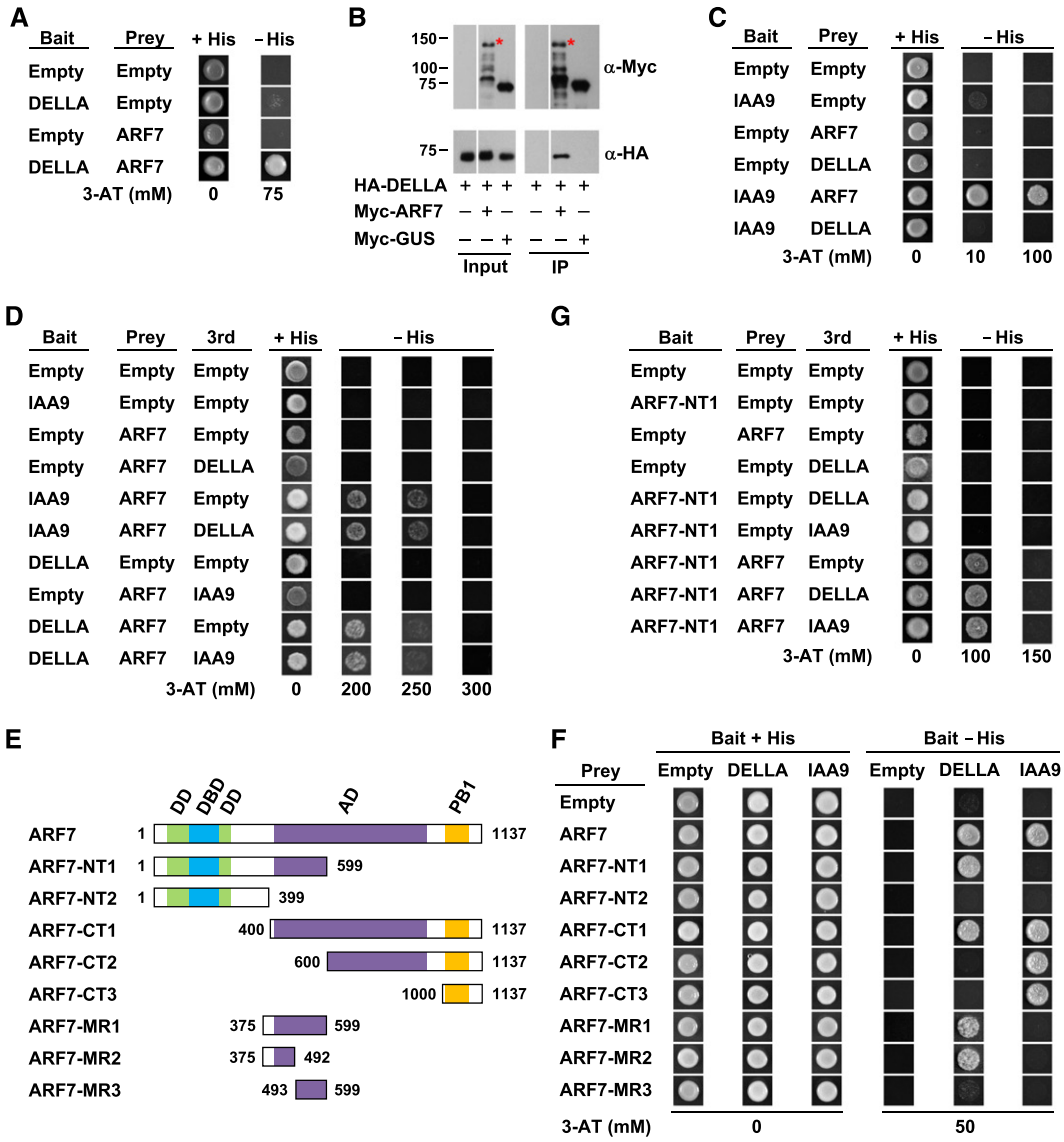

Figure 1. SlARF7 Interacts with SlDELLA and SlIAA9 through Distinct Domains.

(A) Y2H assay showing that SlDELLA directly interacts with SlARF7.
(B) Co-IP of transiently expressed HA-SlDELLA with Myc-SlARF7 or Myc-GUS in *N. benthamiana*. Protein extracts were immunoprecipitated with anti-Myc antibody-conjugated agarose beads. Immunoblot analysis was performed using anti-Myc or anti-HA antibodies. Red asterisk marks the full-length Myc-ARF7, and lower bands are truncated Myc-ARF7.
(C) Y2H assay showing that SlIAA9 interacts with SlARF7, but not with SlDELLA.
(D) DELLA and IAA9 do not compete for binding with ARF7 in a Y3H assay.
(E) Diagram of the full-length and various truncated forms of SlARF7 used in **(F)**. DD, dimerization domain; DBD, DNA binding domain; AD, activation domain; PB1, Aux/IAA binding domain. Numbers refer to amino acids.
(F) SlDELLA and SlIAA9 bind to different regions of SlARF7 in a Y2H assay.
(G) Y3H assay showing that DELLA and IAA9 do not interfere with ARF7 dimerization.
In **(A)**, **(C)**, and **(F)**, +His, synthetic medium minus tryptophan and leucine; –His, synthetic medium minus tryptophan, leucine, and histidine, supplemented with 10, 50, 75, or 100 mM 3-AT, as labeled. In **(D)** and **(G)**, +His and –His media are the same as indicated above, except that uracil was not included in these media. In **(A)**, **(D)**, and **(F)**, DELLA-CT3 (amino acid residues 166–588) was used as the bait.

only when coexpressed with Myc-SlARF7, but not with Myc-GUS or when expressed alone (Figure 1B), thus confirming that SlDELLA and SlARF7 interact in planta.

ARFs, especially the activator subgroup, are known to interact with IAA proteins through their C-terminal PB1 (Phox and Bem1) domains (Vernoux et al., 2011). SlARF7 belongs to the activator subgroup of ARFs. Therefore, we examined whether SlARF7 interacts with SlIAA9, which has been shown to inhibit fruit initiation (Wang et al., 2005). As shown in Figure 1C, SlARF7 interacted strongly with SlIAA9 in a Y2H assay, whereas SlDELLA did not. Furthermore, we performed a yeast three-hybrid (Y3H) assay to test whether SlDELLA and SlIAA9 compete for binding to SlARF7. Neither SlDELLA nor SlIAA9 interfered with the SlARF7-SlIAA9 or SlARF7-SlDELLA interaction, respectively (Figure 1D). These results suggest that SlDELLA and SlIAA9 interact with different regions of SlARF7. To verify this notion, we identified DELLA-interaction domain in SlARF7 using a series of SlARF7 truncation constructs in Y2H assays. As shown in Figures 1E and 1F, amino acid residues 375 to 492 of SlARF7 (ARF7-MR2) are responsible for interacting with DELLA. This region is highly variable among ARFs and is mostly located within the activator/repressor domains (Guilfoyle and Hagen, 2007; Chapman and Estelle, 2009). As expected, the conserved C-terminal PB1 domain of ARF7 (in ARF7-CT3, amino acids 1000–1137) is responsible for binding to IAA9 (Figures 1E and 1F). A recent report revealed a second dimerization domain in ARFs for ARF homodimer formation; this domain flanks the N-terminal DNA binding domain (Boer et al., 2014). Interestingly, the SlDELLA interaction domain in SlARF7 is near this N-terminal ARF dimerization domain (Figure 1E). We therefore tested whether SlDELLA interferes with ARF7 self-dimerization by Y3H assays, using an ARF7-NT1 construct as the bait. Consistent with previous findings (Boer et al., 2014), SlARF7 self-dimerized through its N-terminal region (Figure 1G). However, neither SlDELLA nor SlIAA9 affected SlARF7 self-dimerization in this assay. These results indicate that SlDELLA and SlIAA9 interact with SlARF7 through distinct regions.

Besides *SlARF7*, the tomato genome contains seven additional activator *ARF* genes. However, the available *SlARF6A* sequence only contains a partial coding sequence, and *SlARF6B* is predicted to encode a truncated protein (Zouine et al., 2014). We tested the five remaining SlARFs (i.e., SlARF5, SlARF8A, SlARF8B, SlARF19A, and SlARF19B) by Y2H assays and showed that all of them interacted with SlDELLA and SlIAA9 (Figure 2A). We adopted the same *SlARF* gene names listed in Zouine et al. (2014), with the exception of *SlARF7* and *SlARF19A*/*19B*, which were designated *SlARF19* and *SlARF7A*/*7B*, respectively, in this 2014 report. This is because earlier publications by de Jong et al. (2009) 2011) 2011) already used *SlARF7* for Solyc07g042260.

As described above, neither SlDELLA nor SlIAA9 affected SlARF7 homodimerization in the Y3H assays. Based on sequence homology of their dimerization domains, ARFs were proposed to form heterodimers as well (Boer et al., 2014). We tested whether SlDELLA or SlIAA9 would interfere with ARF heterodimer formation. In a Y3H assay, we found that SlARF7-NT1 formed heterodimers with SlARF8A, SlARF8B, and SlARF19B, respectively. However, coexpression of SlDELLA or SlIAA9 had little effect on these interactions (Supplemental Figure 1).

Downregulation of Multiple Activator *SlARFs* Leads to a Parthenocarpic Phenotype in the *SlARF7 RNAi* Line

Absolute RT-qPCR analysis showed that all activator *SlARFs* were expressed in ovaries around anthesis and that *SlARF5*, *SlARF8A*, and *SlARF8B* were expressed at higher levels than *SlARF7* (Figure 2B; Supplemental Figure 2). However, only *SlARF5* displayed similar temporal expression patterns to those of *SlARF7*: Both *SlARF5* and *SlARF7* were induced at anthesis (0 d after anthesis [DAA]) and downregulated at 3 DAA. We tested whether any of these *SlARFs* (besides *SlARF7*) are downregulated in a previously generated *SlARF7 RNAi* transgenic line (de Jong et al., 2009). As shown in Figure 2C, the mRNA levels of *SlARF5*, *SlARF7*, and *SlARF8B* in 0 DAA ovaries were reduced 40 to 60% in the *SlARF7 RNAi* line compared with the wild type, whereas the expression of the other activator *SlARFs* was not significantly altered. We also analyzed the expression of nine repressor *SlARFs* (*ARF1*, *ARF2A*, *ARF2B*, *ARF3*, *ARF4*, *ARF9A*, *ARF10A*, *ARF16A*, and *ARF24*) that are expressed in 0 DAA wild-type ovaries (http://tomexpress.toulouse.inra.fr/). None of these repressor *SlARFs* showed reduced expression in the *SlARF7 RNAi* line compared with the wild type (Figure 2D). Taken together, the fruit development phenotypes observed in this *SlARF7 RNAi* line are likely caused by the downregulation of *SlARF7*, *SlARF5*, and *SlARF8B*.

To verify the idea that parthenocarpy in the *SlARF7 RNAi* line is caused by the simultaneous downregulation of multiple activator *SlARFs*, we generated an *SlARF7* null mutant (*CR-slarf7*) by CRISPR-Cas9, as well as an *SlARF5* null mutant (*slarf5-1*, also named *slmp-1* because *SlARF5* is most similar to *AtARF5=AtMP*) in the M82 cultivar background. The *CR-slarf7* allele contains a 107-bp deletion (nucleotides 92–198 downstream of the translational start site) in *SlARF7* that leads to an early stop codon after nucleotide 99. The *slarf5-1* allele was identified in an EMS population. This mutant contains a C-to-T (Gln-to-Stop) substitution at nucleotide 754 of the open reading frame downstream of the translational start site, within exon 8. As the *slarf5-1* mutant displayed severe defects in flower development, only the heterozygous mutant (*slarf5*/+) was used to test the parthenocarpic phenotype. We also generated a double mutant that is homozygous for *CR-slarf7* and heterozygous for *slarf5-1* (*arf7 arf5*/+) by genetic crosses. The single mutants *slarf7* and *slarf5*/+ and the double mutant *arf7 arf5*/+ showed normal fruit growth compared with the wild type (Figure 2E). Neither single mutant produced parthenocarpic fruits from emasculated flowers, whereas the double mutant *arf7 arf5*/+ developed parthenocarpy after emasculation (Figures 2E to 2G), indicating that both SlARF5 and SlARF7 are involved in fruit initiation. However, the *CR-slarf7 slarf5*/+ double mutant produced parthenocarpic fruits at a lower frequency than the *ARF7 RNAi* line. These results suggest that the parthenocarpic phenotype of the *SlARF7 RNAi* line is caused by downregulation of multiple activator *SlARFs*. The *SlARF7 RNAi* line, with its clear parthenocarpic phenotype, represents a valuable tool for studying the role of the SlDELLA-SlARF interaction in fruit set.

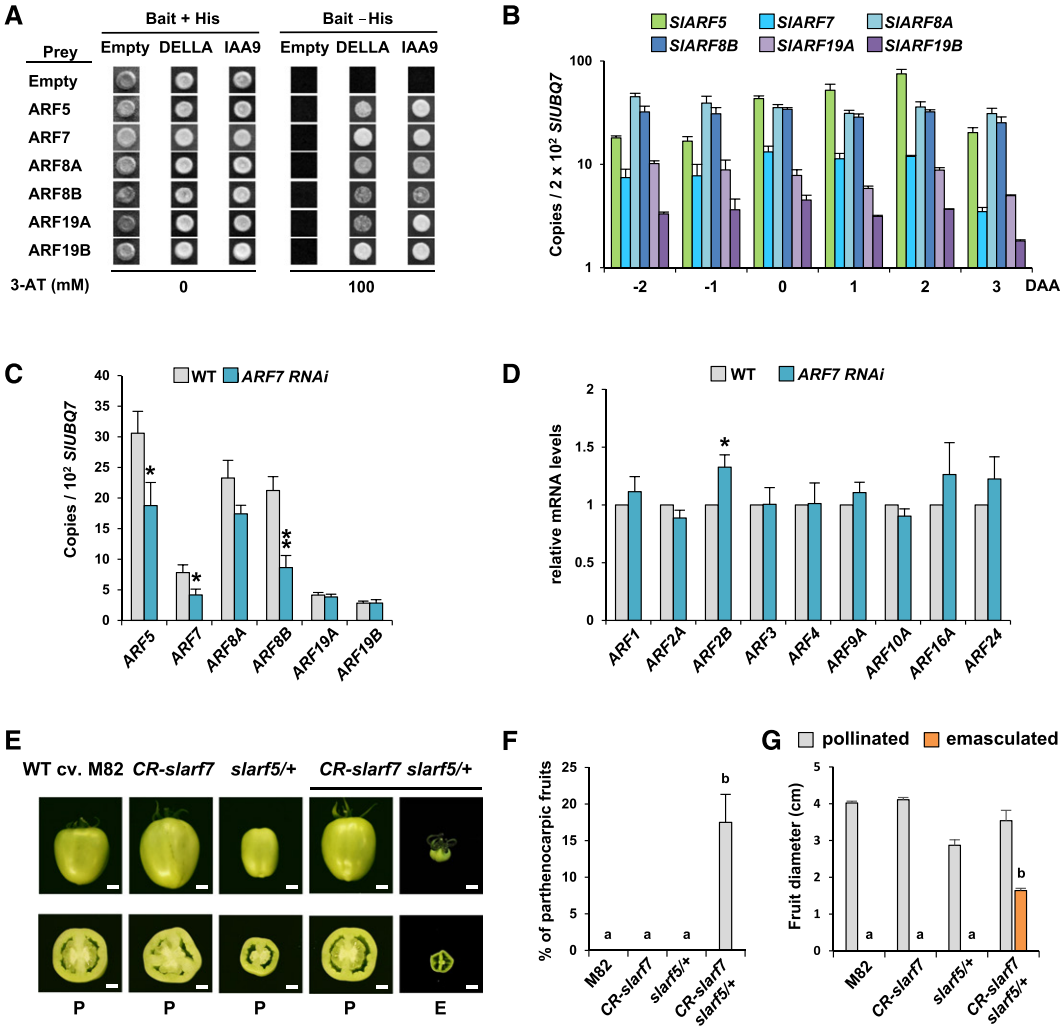

Figure 2. Several Activator SlARFs Likely Function in Fruit Set.

(A) Activator SlARFs interact with SlDELLA and SlIAA9 in a Y2H assay. DELLA-CT3 (amino acid residues 166–588) was used as the bait. +His, synthetic medium minus tryptophan and leucine; –His, synthetic medium minus tryptophan, leucine, and histidine.

(B) Temporal expression patterns of activator *SlARFs* in ovaries around anthesis. Absolute transcript levels of activator *SlARFs* in wild-type (MM) ovaries from –2 to +3 DAA.

(C) Absolute transcript levels of activator *SlARFs* in 0 DAA ovaries of the wild type and the *SlARF7 RNAi* line. The mRNA levels in **(B)** and **(C)** were calculated using standard curves (Supplemental Figure 2) and are shown as the number of copies of *SlARF* cDNA per 2×10^2 and 10^2 copies of *SlUBQ7*, respectively.

(D) Repressor *SlARFs* are not downregulated in the *SlARF7 RNAi* line. Relative repressor *SlARF* mRNA levels in wild-type or *ARF7 RNAi* 0 DAA ovaries were determined by RT-qPCR analysis. *SlUBQ7* was used to normalize different samples. The level of each repressor *SlARF* in the wild type was set to 1. In **(B)** to **(D)**, means ± SE of three biological replicates from independent pools of tissues (two technical repeats each) are shown. *P < 0.05 and **P < 0.01.

(E) to **(G)** The *CR-slarf7 slarf5*/+ double mutant produces parthenocarpic fruits. In **(E)**, photographs were taken 4 weeks after pollination (P) or emasculation (E). Bar = 1 cm. In **(F)**, parthenocarpy efficiency was calculated as percentage of parthenocarpic fruits that developed from emasculated flowers. In **(G)**, average sizes of fruits from pollinated and emasculated wild-type and mutant flowers are shown. In **(F)** and **(G)**, means ± SE from three biological repeats (sampled at different times). *n* = 21 to 85 for each line. Different letters above bars represent significant differences among emasculated lines, P < 0.01.

SlDELLA and SlARF7/SlIAA9 Antagonistically Regulate the Expression of GA/Auxin Feedback-Regulated Genes

Our finding that SlDELLA directly interacts with the activator SlARFs suggests that these key regulatory proteins may coordinate GA and auxin signaling activity during fruit initiation and development. In the rest of this report, we mainly focused on the interaction between SlARF7 and SlDELLA. To investigate whether and how the SlDELLA-SlARF7 interaction controls the expression of common target genes, we analyzed the transcript levels of early GA-responsive genes (*SlGA20ox1* and *SlGA3ox1*; Serrani et al., 2008) and auxin-responsive genes (*SlGH3.2*; Kumar et al., 2012) in

ovaries of wild-type tomato flowers at –1 DAA. These genes were chosen because they are likely the direct targets of SlDELLA and/or SlARFs. The use of –1 DAA ovaries allowed us to examine the effects of auxin and GA on the expression of these genes. Flower morphology around anthesis is shown in Figure 3A. *SlGA20ox1*, *SlGA3ox1*, and *SlGH3.2* were repressed by GA application compared with mock treatment (Figure 3B). By contrast, treatment with 2,4-D (a synthetic auxin analog) induced the expression of all three genes (Figure 3C). To test whether *GA20ox1*, *GA3ox1*, and *GH3.2* are common targets of DELLA/ARF7-IAA9 during early GA/auxin signaling, we examined the expression of these genes in loss of function or reduced expression mutants of *SlDELLA*, *SlARF7*, and *SlIAA9*. Consistently, *GA20ox1*, *GA3ox1*, and *GH3.2* expression was reduced in *procera* (*pro*; a *SlDELLA* loss-of-function mutant) but increased in the *SlARF7 RNAi* line and *entire* (*SlIAA9* loss-of-function mutant) compared with the wild type (Figures 3D and 3E), indicating that SlDELLA activates the expression of these genes while SlARF7 and SlIAA9 repress their expression. GH3.2 belongs

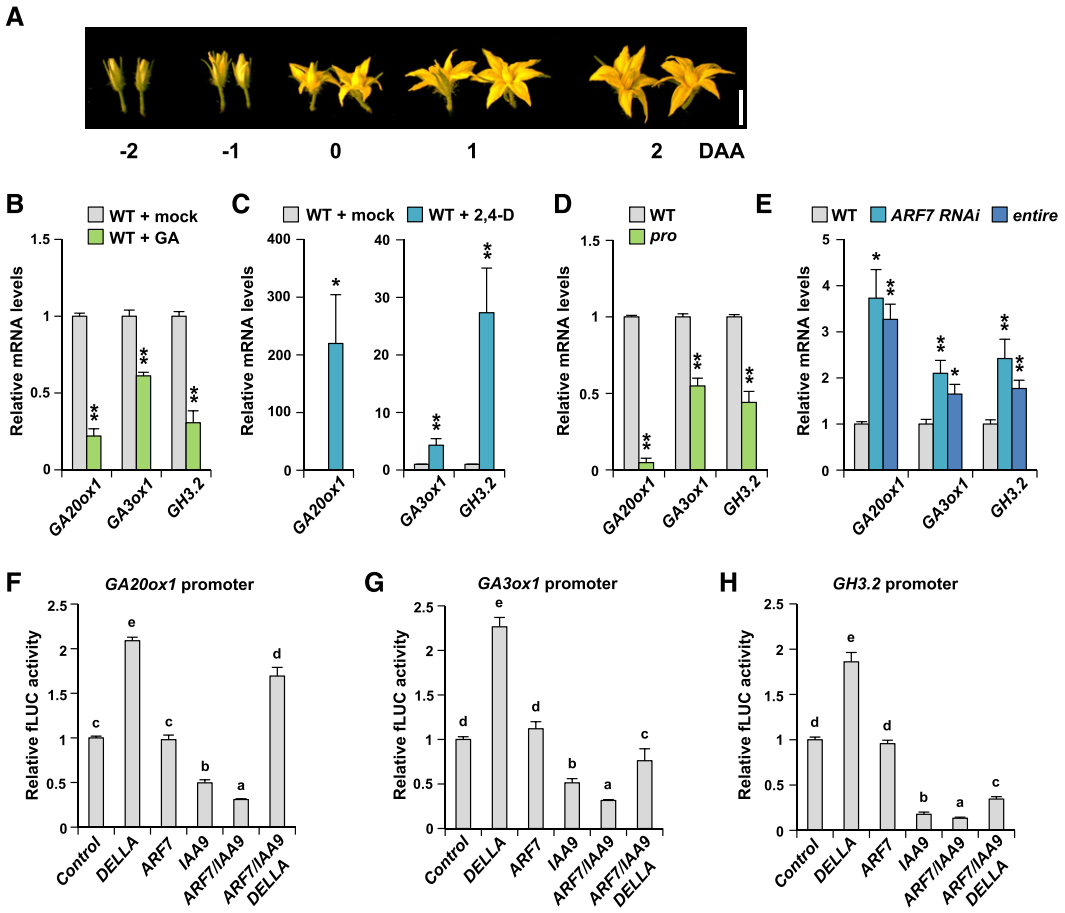

Figure 3. SlDELLA and SlARF7/SlIAA9 Antagonistically Regulate GA- and Auxin-Feedback-Regulated Genes.

(A) Wild-type flower morphology around anthesis is similar to that described previously (Brukhin et al., 2003). Flowers were harvested from wild-type plants at different developmental stages without further manipulation. Bar = 1 cm.

(B) to **(E)** Relative mRNA levels in –1 DAA ovaries, as determined by RT-qPCR analysis. The housekeeping gene, *SlUBQ7*, was used to normalize different samples. Means ± SE of three biological replicates from independent pools of tissues (two technical repeats each) are shown. The level in mock treatment (**[B]** and **[C]**) or the wild type (**[D]** and **[E]**) was set to 1. *P < 0.05 and **P < 0.01. In **(B)** and **(C)**, –1 DAA ovaries of emasculated flowers were treated with hormone or mock treated.

(B) and **(D)** GA biosynthetic genes (*GA20ox1* and *GA3ox1*) and amino acid-auxin conjugating gene (*GH3.2*) were repressed after 6 h GA_3 treatment and in the *pro* mutant (compared with that in the wild type).

(C) and **(E)** *GA20ox1*, *GA3ox1*, and *GH3.2* were induced after 6 h 2,4-D treatment **(C)** and in elevated auxin-signaling mutants *ARF7 RNAi* and *entire* (*iaa9*) **(E)**.

(F) to **(H)** Dual luciferase assay in the *N. benthamiana* transient expression system showing that SlDELLA and SlARF7/SlIAA9 antagonistically regulate the expression of *GA20ox1* **(F)**, *GA3ox1* **(G)**, and *GH3.2* **(H)**. Means ± SE of nine biological replicates are shown. Different letters above the bars represent significant differences (P < 0.01). The reporter constructs contained the 2.5-kb *GA20ox1* promoter **(F)**, 2.4-kb *GA3ox1* promoter **(G)**, and 2.5-kb *GH3.2* promoter **(H)** fused to the *fLUC* coding sequence. Effector constructs used in each assay are as labeled, and the empty effector construct was included as a negative control.

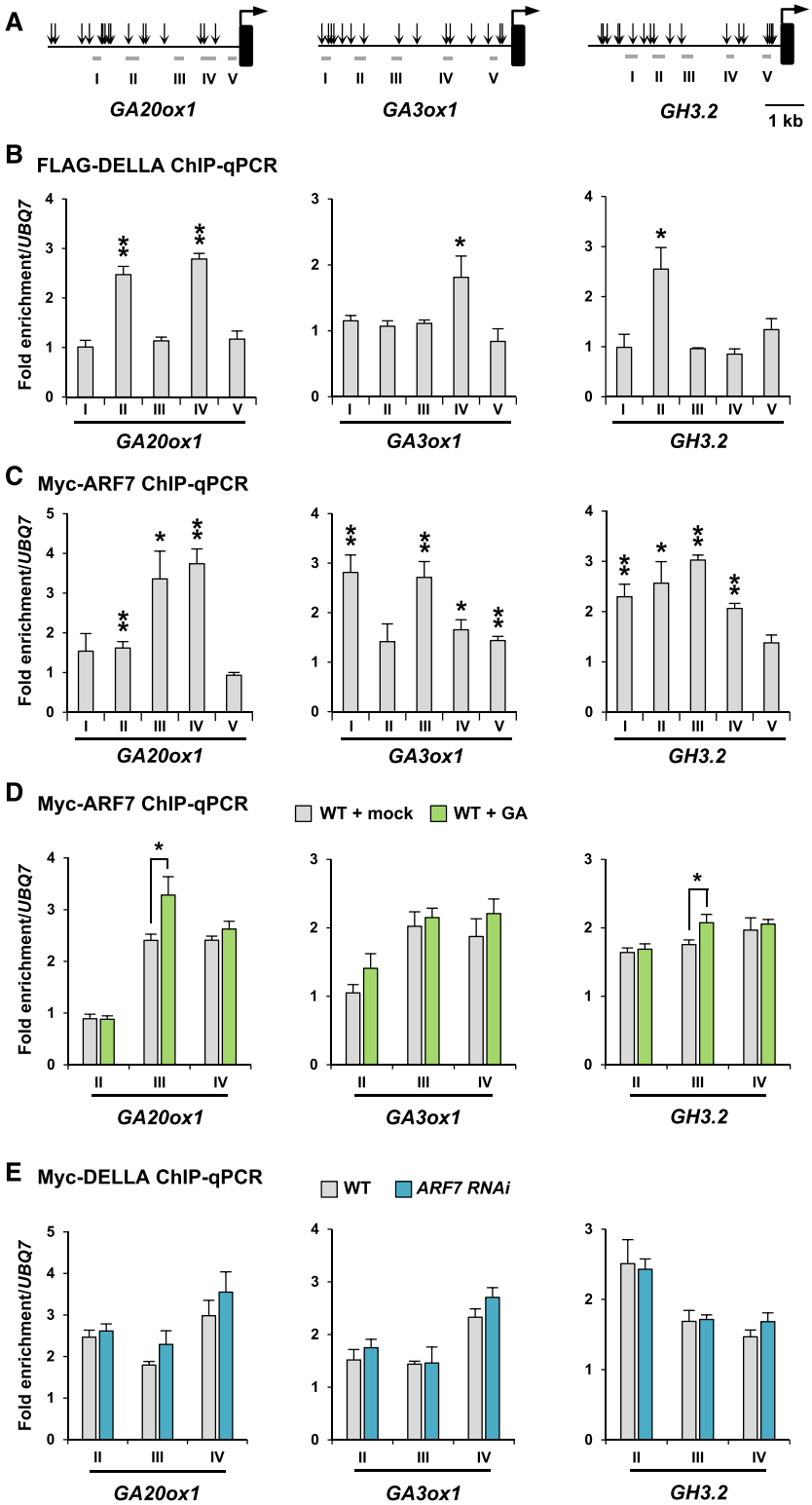

Figure 4. Direct Association of SlDELLA and SlARF7 with the Promoters of GA/Auxin Feedback-Regulated Genes Revealed by ChIP-qPCR.

(A) Diagrams of the *SlGA20ox1*, *SlGA3ox1*, and *SlGH3.2* promoters. qPCR amplicons for ChIP-qPCR are depicted as short lines under the promoters. The downward arrow points to the position of the canonical AuxRE (TGTC) elements in these promoters. The bent arrow indicates translational start sites.

to group II of the GH3 protein family; some group II members in Arabidopsis and rice are auxin-amino acid conjugating enzymes that convert auxin to an inactivate form (Staswick et al., 2005; Park et al., 2007). Thus, our result suggests that GA may regulate auxin homeostasis through GH3.2. However, some members of the GH3 family conjugate amino acids to jasmonic acid or salicylic acid instead of auxin (Staswick et al., 2002). To investigate whether auxin can serve as a substrate for GH3.2, we performed an in vitro enzyme assay using GST-GH3.2 protein produced in *Escherichia coli*. As shown in Supplemental Figure 3, GST-GH3.2 conjugated aspartic acid to IAA, but GST alone did not, suggesting that GH3.2 is an auxin-amino acid conjugating enzyme.

Because the transcript levels of *SlGA20ox1*, *SlGA3ox1*, and *SlGH3.2* in –1 DAA ovaries were reduced in *pro* compared with the wild type and increased in *SlARF7 RNAi* and *entire* (Figures 3D and 3E), we hypothesized that the SlARF7-SlIAA9 complex represses the transcription of *SlGA20ox1*, *SlGA3ox1*, and *SlGH3.2*, whereas SlDELLA induces the expression of these genes by interacting with SlARF7. In the absence of SlIAA9, SlARF7 may act as a transcriptional activator either as a homodimer or heterodimer with other ARFs, as it contains a glutamine-rich sequence and is predicted to be a transcriptional activator (de Jong et al., 2009). To test this possibility, SlDELLA, SlARF7, and SlIAA9 were transiently expressed alone or coexpressed in *N. benthamiana* leaves by agroinfiltration to determine whether they compete to modulate the transcription of *SlGA20ox1*, *SlGA3ox1*, and *SlGH3.2* using a dual luciferase (LUC) reporter assay. The reporter constructs contained promoter sequences of *GA20ox1*, *GA3ox1*, and *GH3.2*, which were fused to the firefly *LUC* gene (*fLUC*). The Pro_{35S}*:Renilla LUC* (*rLUC*) construct was used as an internal standard. Three effectors, Pro_{35S}*:SlDELLA*, Pro_{35S}*:SlARF7*, and Pro_{35S}*:SlIAA9*, were included in the assays. As shown in Figures 3F to 3H, SlDELLA alone induced transcription of these target genes, while SlIAA9 repressed their transcription, which is consistent with the above in vivo expression data. SlARF7 alone did not alter the expression of these three genes. However, when combined with SlIAA9, SlARF7 caused further repression of the target genes compared with SlIAA9 alone (Figures 3F to 3H), suggesting that SlARF7 may recruit SlIAA9 to these promoters for transcriptional repression. Coexpression of SlDELLA with SlARF7 and SlIAA9 resulted in intermediate fLUC activity (lower than that in the SlDELLA alone sample, but higher than the SlARF7/SlIAA9 sample). These results strongly suggest that through an interaction with SlARF7, SlDELLA antagonizes the repressive effect of SlARF7/SlIAA9 on these target genes, which are under feedback regulation and are important for GA and auxin homeostasis.

We then performed chromatin immunoprecipitation-quantitative PCR (ChIP-qPCR) to determine whether SlDELLA and SlARF7 bind directly to the promoters of these feedback-regulated target genes in vivo. For ChIP of SlDELLA binding sites, we generated a transgenic tomato line containing $Pro_{SlDELLA}$*:FLAG-SlDELLA* in the *pro* mutant background. In this line, the FLAG-SlDELLA fusion protein is functional as it rescued the overall phenotypes of *pro*, including stem growth, leaf shape, and fruit development (Supplemental Figures 4A to 4D). In addition, FLAG-SlDELLA is responsive to GA-induced degradation (Supplemental Figure 4E). Using –1 DAA ovaries from the *FLAG-SlDELLA* line, cross-linked chromatin was pulled down using anti-FLAG beads, and qPCR was performed on several primer pairs that span the promoter region of each feedback-regulated target gene (Figure 4A). *SlUBQ7* was used to normalize the qPCR results in each ChIP sample. A 1.8- to 2.8-fold enrichment was observed for promoter sequences of *GA20ox1*, *GA3ox1*, and *GH3.2* (Figure 4B). To test whether SlARF7 also binds to these promoters, we transiently expressed a Myc-SlARF7 construct in developing tomato fruits by agroinfiltration because the stable transgenic line was not available. When we performed ChIP using anti-Myc beads, a 2.8- to 3.7-fold enrichment of promoter sequences of these target genes was observed by qPCR (Figure 4C). These results indicate that both SlDELLA and SlARF7 directly associate with the promoters of these target genes.

To examine whether SlDELLA interferes with the binding of SlARF7 to the promoters of these feedback-regulated genes, we pretreated wild-type plants with PAC for 2 weeks and transiently expressed Myc-SlARF7 in developing fruits, followed by GA or mock treatment. Immunoblot analysis indicated that SlDELLA protein levels were enhanced by PAC and that GA treatment dramatically reduced SlDELLA protein levels (Supplemental Figure 5). ChIP-qPCR showed that GA treatment slightly increased SlARF7 binding to *GA20ox1* and *GH3.2* promoters compared with the mock-treated control (Figure 4D). These results suggest that the SlDELLA-SlARF7 interaction inhibits the binding of SlARF7 to these target promoters. On the other hand, when transiently expressed in fruits of the wild type or *SlARF7 RNAi*, Myc-DELLA protein bound to its feedback-regulated target genes to similar levels in these plants, as shown by ChIP-qPCR (Figure 4E). These results suggest that the reduced SlARF7 level in *SlARF7 RNAi* had no obvious effect on the association of DELLA with its target promoters.

Figure 4. (continued).

(B) SlDELLA binds to the promoter regions of *GA20ox1*, *GA3ox1*, and *GH3.2* in vivo. Chromatin isolated from cross-linked –1 DAA ovaries of the $Pro_{SlDELLA}$*:FLAG-SlDELLA* transgenic tomato line was immunoprecipitated using anti-FLAG antibodies followed by qPCR.

(C) Myc-SlARF7 binds to GA and auxin feedback-regulated genes, as determined by ChIP-qPCR. Pro_{35S}*:Myc-SlARF7* was transiently expressed in tomato fruits by agroinfiltration, and ChIP was performed using anti-Myc antibodies followed by qPCR.

(D) ChIP-qPCR analysis showing that GA treatment enhances SlARF7 binding to the *GA20ox1* and *GH3.2* promoters, presumably due to reduced DELLA protein levels. Myc-ARF7 was transiently expressed as in **(C)**.

(E) Myc-SlDELLA transiently expressed in the wild type or the *SlARF7 RNAi* line shows equal binding to the promoters of feedback-regulated genes, as determined by ChIP-qPCR analysis.

In **(B)** to **(E)**, the relative enrichment was calculated by normalizing against ChIP-qPCR of nontransgenic control samples using *SlUBQ7*. The normalized values of fold enrichment are the average ± SE of three biological replicates from independent pools of tissues. *$P < 0.05$ and **$P < 0.01$.

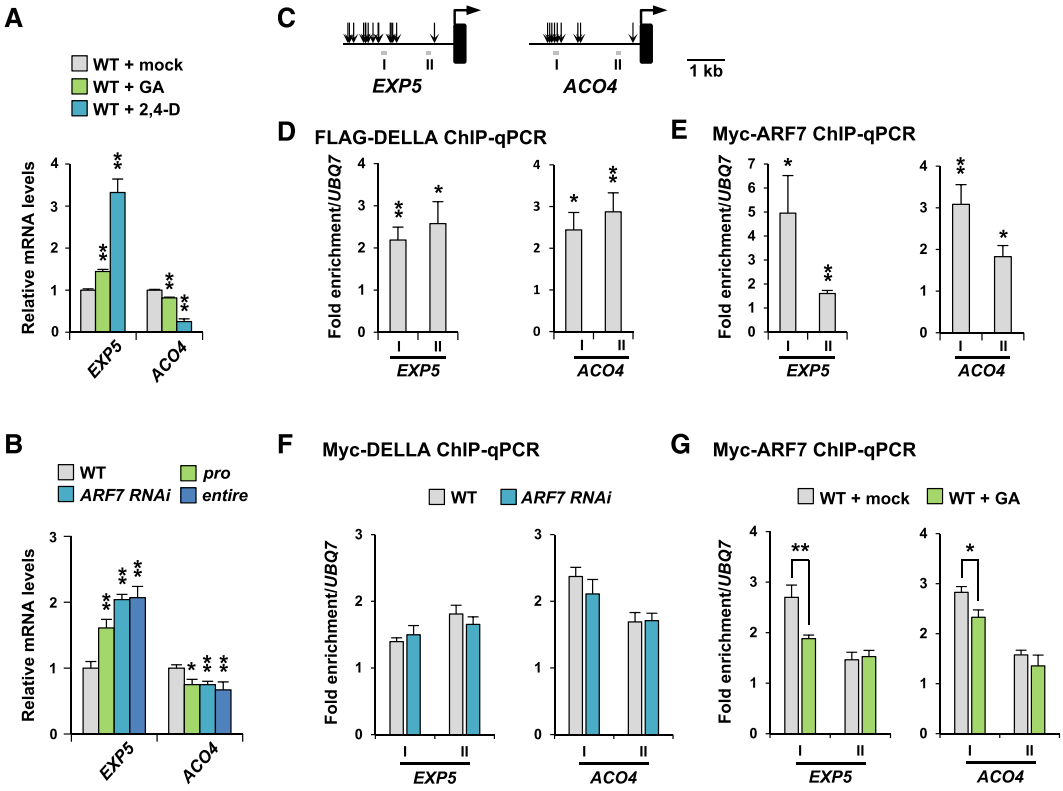

Figure 5. SlDELLA and SlARF7/SlIAA9 Have Similar Effects on Their Direct Downstream Target Genes, *EXP5* and *ACO4*.

(A) and **(B)** Relative mRNA levels in –1 DAA ovaries, as determined by RT-qPCR analysis. The housekeeping gene, *SlUBQ7*, was used to normalize different samples. Means ± SE of three biological replicates (two technical repeats each) are shown. The level in mock treatment **(A)** or the wild type **(B)** was set to 1. *P < 0.05 and **P < 0.01. *EXP5* was induced after 6 h GA_3 or 2,4-D treatment **(A)** and in the *pro*, *ARF7 RNAi*, and *entire* (*iaa9*) mutants (**[B]**; compared with that in the wild type). By contrast, *ACO4* was repressed by GA_3 or 2,4-D treatment **(A)** and in *pro*, *ARF7 RNAi*, and *entire* (*iaa9*) mutants **(B)**.

(C) Diagrams of the *SlEXP5* and *SlACO4* promoters. qPCR amplicons for ChIP-qPCR are labeled as short lines under each diagram. The downward arrow points to the position of the canonical AuxRE (TGTC) elements in these promoters. The bent arrow indicates translational start sites.

(D) SlDELLA binds to the promoter regions of *EXP5* and *ACO4* in vivo, as revealed by ChIP-qPCR analysis. Chromatin isolated from cross-linked –1 DAA ovaries of the $Pro_{SlDELLA}$*:FLAG-SlDELLA* tomato line was immunoprecipitated using anti-FLAG antibodies followed by qPCR.

(E) Binding of transiently expressed Myc-SlARF7 to *EXP5* and *ACO4*, as determined by ChIP-qPCR. Pro_{35S}*:Myc-SlARF7* was transiently expressed in tomato fruits by agroinfiltration, and ChIP was performed using anti-Myc antibodies followed by qPCR.

(F) Myc-SlDELLA transiently expressed in the wild type or the *SlARF7 RNAi* line shows equal binding to the promoters of downstream target genes, as determined by ChIP-qPCR analysis.

(G) ChIP-qPCR analysis showing that GA treatment reduces SlARF7 binding to the *EXP5* and *ACO4* promoters, presumably due to reduced DELLA protein levels. Myc-ARF7 was transiently expressed as in **(E)**.

In **(D)** to **(G)**, the relative enrichment was calculated by normalizing against ChIP-qPCR of nontransgenic control samples using *SlUBQ7*. The normalized values of fold enrichment are the average ± SE of three biological replicates from independent pools of tissues. *P < 0.05 and **P < 0.01.

SlDELLA and SlARF7/SlIAA9 Coregulate Downstream Target Genes in Developing Fruits

Although SlDELLA and SlARF7/SlIAA9 play opposite roles in modulating the expression of feedback-regulated genes involved in GA and auxin metabolism, mutations in *SlIAA9* and *SlDELLA*, as well as the downregulation of *SlARF7* together with additional related ARF genes, lead to fertilization-independent fruit initiation. Therefore, it is possible that SlDELLA and SlARF7/SlIAA9 coregulate common downstream target genes that control fruit initiation in response to GA and auxin signals. Tang et al. (2015) performed transcriptome profiling of GA- and auxin-induced parthenocarpic tomato fruit at 4 d after hormone treatments. Importantly, the expression of a number of genes is regulated similarly by both hormones, making them candidates for early fruit development genes that are coregulated by SlDELLA and SlARF7/SlIAA9. To test this idea, we analyzed the expression of 14 selected genes in –1 DAA wild-type ovaries to determine whether they are coregulated by GA and auxin at 6 and 24 h after treatment (Supplemental Figure 6). Among these, 10 genes, including *EXPANSIN5* (*EXP5*, Solyc02g088100) and *ACC OXIDASE4* (*ACO4*, Solyc02g081190), were coregulated by GA and auxin at these early time points. *EXP5* likely promotes cell expansion during fruit development. *ACO4* is an

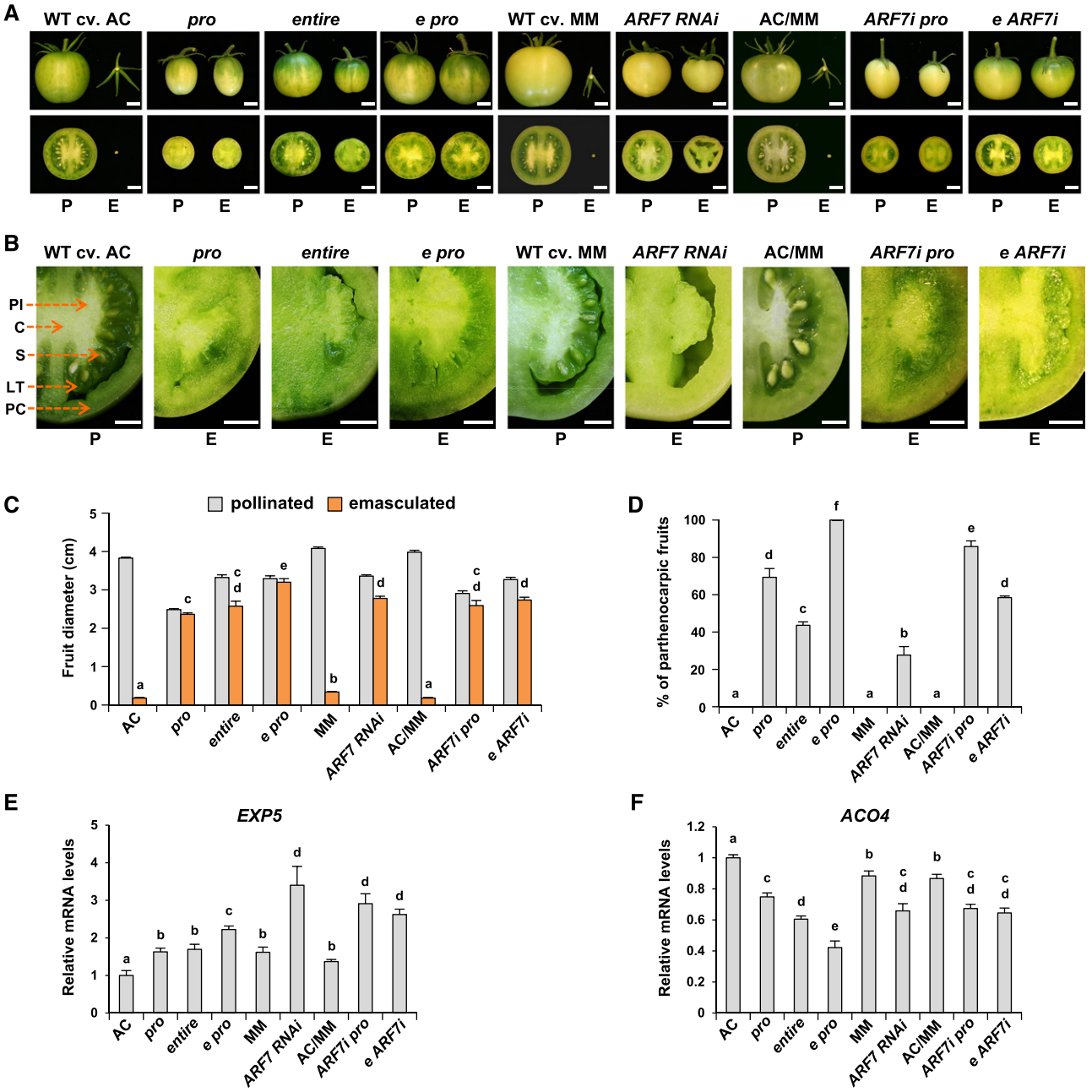

Figure 6. SlDELLA, SlARF7, and SlIAA9 Additively Repress Fruit Initiation and Growth.

(A) and **(B)** Parthenocarpic growth in *pro*, *entire*, and *ARF7 RNAi* single and double mutants. WT cv. AC, Ailsa Craig; MM, Moneymaker; AC/MM, AC/MM hybrid. Photographs were taken 4 weeks after pollination (P) or emasculation (E). Pericarp (PC), locule tissue (LT), seed (S), placenta (Pl), and columella (C). Bars = 1 cm in **(A)** and 0.5 cm in **(B)**.

(C) Average sizes of fruits from pollinated and emasculated wild-type and mutant flowers. Means ± SE (*n* = 26–32 for pollinated fruits; 17–20 for parthenocarpic fruits). Different letters above bars represent significant differences among parthenocarpic fruits, $P < 0.01$.

(D) Parthenocarpy efficiency as calculated by percentage of parthenocarpic fruits that developed from emasculated flowers. Means ± SE. *n* = 18 to 28 for most lines, but *n* = 41 to 50 for mutants with low parthenocarpy efficiency, including *ARF7 RNAi*, *entire*, and *e ARF7i*. Different letters above bars represent significant differences, $P < 0.05$.

(E) and **(F)** Transcript levels of *EXP5* and *ACO4* in –1 DAA ovaries of single and double mutants. Means ± SE of three biological replicates (two technical repeats each) are shown. Different letters above bars represent significant differences ($P < 0.01$).

ethylene biosynthesis gene, which may regulate fruit set because ethylene inhibits this process (Vriezen et al., 2008; Shinozaki et al., 2015). Figure 5A shows that *EXP5* was induced by 6 h of GA and auxin treatment, while *ACO4* was repressed by both hormones. Consistently, *EXP5* was upregulated in *pro*, *ARF7 RNAi*, and *entire* mutants, while *ACO4* was downregulated in all three lines (Figure 5B). Therefore, SlDELLA and SlARF7/SlIAA9 have similar effects on *EXP5* and *ACO4* expression. ChIP-qPCR analysis showed that both SlDELLA and SlARF7 are associated with the promoters of these two genes in vivo (Figures 5C to 5E), indicating that *EXP5* and *ACO4* are direct targets of SlDELLA and SlARF7. We then tested whether DELLA levels affect the binding of SlARF7 to these target promoters by ChIP-qPCR analysis. Wild-type plants were pretreated with PAC before Myc-SlARF7 was transiently expressed in developing fruits, followed by GA or mock treatment. ChIP-qPCR analysis showed that SlARF7 displayed slightly reduced binding to the *EXP5* and *ACO4* promoters in GA-treated sample (Figure 5G), suggesting that the SlARF7-SlDELLA interaction may enhance SlARF7 binding to these target promoters. By contrast, the association of Myc-SlDELLA with these promoters was not affected by reduced levels of activator SlARFs in the *SlARF7 RNAi* lines compared with that in the wild type (Figure 5F). Thus, the association of SlDELLA with these promoters does not depend on SlARF7.

Additive Interactions among *pro*, *SlARF7 RNAi* (Downregulation of Multiple Activator SlARFs), and *entire* (*iaa9*) Mutations during Parthenocarpic Fruit Development

To further investigate the effects of the SlDELLA and SlARFs/SlIAA9 interaction on fruit set and growth, we generated double homozygous mutants by genetic crosses using *pro*, *SlARF7 RNAi*, and *entire* mutant lines. The *SlARF7 RNAi* line was used in this genetic analysis because it displays a clear parthenocarpic fruit phenotype due to the downregulation of several activator *SlARFs* (*SlARF5*, *SlARF7*, and possibly *SlARF8B*). We compared the fruit phenotypes of these single and double mutants, including fruits produced after self-pollination and parthenocarpic fruits from emasculated flowers, to those of the single mutants and wild-type plants. Because *pro* and *entire* are in the Ailsa Craig (AC) background, while the *SlARF7 RNAi* line is in the Moneymaker (MM) background, we included both the AC and MM cultivars and the hybrid AC/MM (F1 of AC × MM) as wild-type controls in these experiments. The *entire* (*e*) and *pro* mutations in the *e pro* double mutant displayed additive effects in terms of parthenocarpic fruit development compared with *entire* and *pro* single mutants (Figures 6A and 6B). The parthenocarpic fruits (from emasculated flowers) of the *e pro* double mutant had more advanced fruit structure compared with the other lines, including further developed placenta, locule tissues, and pseudoembryos (Figures 6A and 6B), as well as larger fruit size (Figure 6C). By contrast, *SlARF7 RNAi pro* (*ARF7i pro*) and *entire SlARF7 RNAi* (*e ARF7i*) double mutants mainly showed additive effects in terms of growth in the placenta and locule tissues (Figures 6A and 6B), with unaltered fruit size (Figure 6C). Nevertheless, when we measured the efficiency of parthenocarpy formation (i.e., percentage of parthenocarpic fruits that formed versus total ovaries emasculated), all three double mutants showed significantly higher efficiency than their corresponding single mutants (Figure 6D). These results, together with our biochemical data, support the notion that crosstalk between GA and auxin occurs during fruit initiation through interactions among SlDELLA, SlARFs, and SlIAA9. Furthermore, we analyzed the expression of their coregulated downstream target genes in the double mutants. In *e pro*, *EXP5* and *ACO4* were more highly induced or repressed, respectively, than those in the single mutants (Figures 6E and 6F). Overall, the results from double mutant phenotyping and target gene analysis support the idea that the interaction of SlDELLA with SlARFs/SlIAA9 has an important impact on their downstream target genes, as well as fruit set and subsequent growth.

Active GA Biosynthesis and Signaling Is a Prerequisite for Tomato Fruit Initiation

A previous study suggested that auxin induces parthenocarpy in tomato via GA-dependent and -independent pathways (Serrani et al., 2008). This model is based on the observation that treatment with the GA biosynthesis inhibitor, PAC, did not block auxin-induced tomato fruit initiation, but it only partially inhibited parthenocarpic fruit growth (Serrani et al., 2008). However, depending on the treatment conditions, PAC treatment may not completely block GA biosynthesis and could have nonspecific effects. To verify the current model, we used the severe GA-deficient tomato mutant *gib1* to test the effect of auxin on parthenocarpy. The *gib1* mutant is impaired in the first committed step in GA biosynthesis, which is catalyzed by *ent*-copalyl diphosphate synthase (Bensen and Zeevaart, 1990). *GIB1* has been mapped to chromosome 6 (Koornneef et al., 1990). However, the molecular lesion in the *gib1* mutant has not been reported. By performing BLAST searches using the AtCPS protein sequence as a query, we identified *Solyc06g084240* as a putative *SlCPS.* This locus is indeed labeled as *CPS1* in the Sol Genomics Network website (https://solgenomics.net/). DNA sequence analysis showed that the *SlCPS* cDNA from the *gib1* mutant contains a deletion of G at nucleotide 563 (from the ATG start site), which leads to four new amino acids after amino acid 187, followed by a premature stop codon. Further sequencing of the nearby genomic region in *gib1* revealed that instead of a deletion, there is a G-to-A mutation at the end of intron 4 (nucleotide 1178 from the start codon). This mutation shifted the intron excision site one nucleotide into exon 5 (from TA**G**|GAA to TA**A**G|AA, where | indicates a splicing site). Taken together, we confirmed that *gib1* is a loss-of-function allele of *SlCPS* (*Solyc06g084240*).

Consistent with previous studies (Serrani et al., 2007, 2008), in wild-type plants, GA or auxin treatment of emasculated −1 DAA ovaries promoted seedless fruit growth (Figure 7A). To understand the role of GA in these responses, we tested how −1 DAA *gib1* ovaries respond to GA and 2,4-D treatment after emasculation. As shown in Figures 7B and 7C, 3 weeks after auxin treatment, *gib1* ovaries were the same size as mock-treated ovaries. By contrast, GA treatment dramatically promoted parthenocarpic fruit development in *gib1*. Cross sections of mock- versus auxin-treated *gib1* ovaries showed similar pericarp and placenta structures, further supporting the observation that auxin failed to promote seedless fruit set in *gib1* (Figure 7D). To rule out the

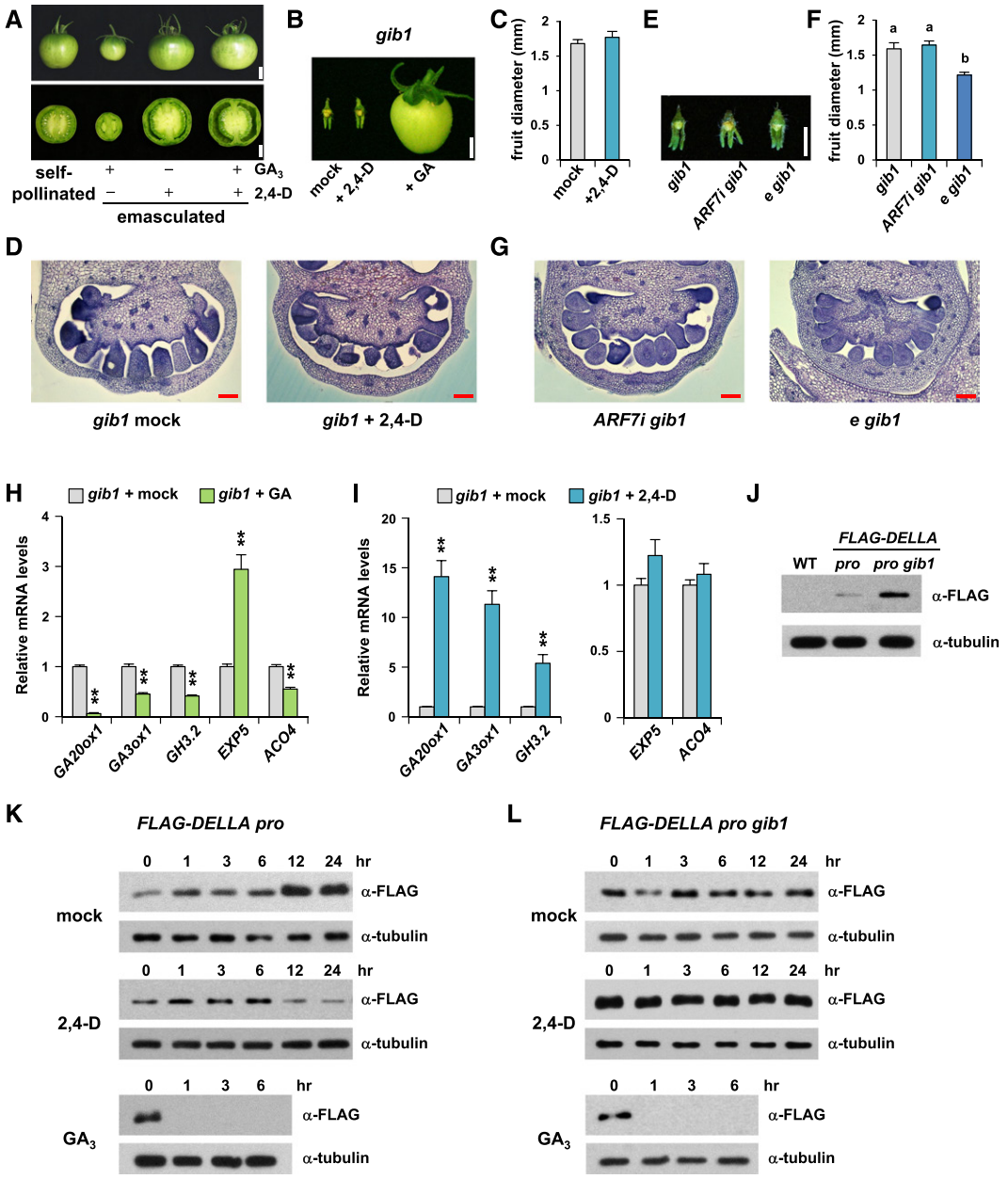

Figure 7. The Induction of Fruit Initiation by Auxin Requires Active GA Signaling.

(A) Parthenocarpy is induced by exogenous application of GA and/or auxin in wild-type –1 DAA ovaries. Photographs were taken 3 weeks after pollination or emasculation + hormone treatment (bar = 1 cm).

(B) to **(D)** In the GA biosynthetic mutant *gib1*, parthenocarpy is induced by the application of GA_3, but not 2,4-D. –1 DAA ovaries of emasculated flowers were treated with mock solution or hormones as indicated. Three weeks after treatment, photographs of ovaries/fruits were taken **(B)**, average diameters of ovaries were measured **(C)**, and cellular structures were analyzed by cross sectioning **(D)**. Bars = 1 cm in **(B)** and 100 μm in **(D)**. In **(C)**, means ± SE (n = 16).

(E) to **(G)** *ARF7i gib1* and *e gib1* double mutants are unable to produce parthenocarpic fruits. Flowers were emasculated at –1 DAA. Five weeks after emasculation, photographs were taken ([E]; bar = 5 mm), and fruit diameters were measured **(F)**. In **(F)**, means ± SE (n = 30), and different letters above bars represent significant differences ($P < 0.01$). Cellular structures were analyzed by cross sectioning **([G]**; bar = 100 μm).

(H) and **(I)** In *gib1*, DELLA/ARF7/IAA9 downstream target genes (*EXP5* and *ACO4*) did not respond to 2,4-D treatment **(I)**, while feedback-related genes did. By contrast, all genes responded to GA_3 in the same manner as in the wild type **(H)**. Values are means ± SE of three biological replicates (two technical repeats each). **$P < 0.01$.

(J) FLAG-DELLA protein accumulates to a higher level in *pro gib1* than in the *pro* background.

(K) The application of 2,4-D to emasculated –1 DAA ovaries of *FLAG-DELLA pro* reduced SIDELLA protein levels gradually over a 24-h period. DELLA

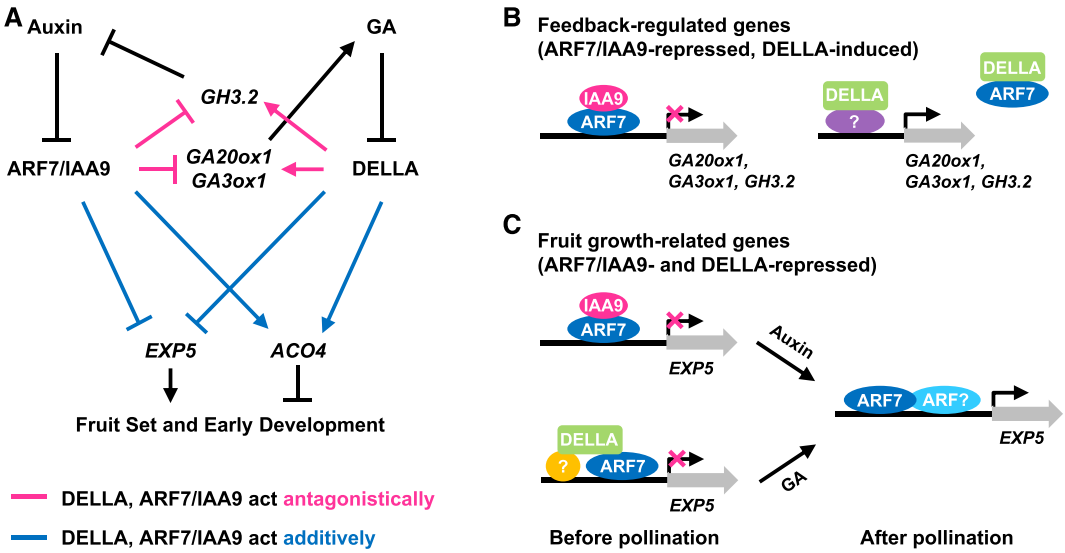

Figure 8. Model of the Crosstalk between the Early GA and Auxin Signaling Pathways during Tomato Fruit Initiation.

(A) Schematic of the GA and auxin pathways. The SlARF7/SlIAA9 complex functions as an auxin signaling repressor complex, and SlDELLA is a GA signaling repressor. These proteins additively inhibit tomato fruit set and fruit development by repressing the expression of growth-related genes (e.g., *EXP5*) and activating ethylene biosynthesis gene (*ACO4*). By contrast, SlARF7/SlIAA9 and SlDELLA antagonistically regulate the expression of feedback-regulated genes, including GA biosynthesis genes (*GA20ox1* and *GA3ox1*) and auxin deactivation gene (*GH3.2*). Upon pollination, auxin and GA play key roles in fruit set. Auxin levels increase in the fertilized ovule, which in turn induces IAA9 degradation and GA biosynthesis. Elevated GA levels then trigger SlDELLA degradation. Removing both SlDELLA and SlIAA9 promotes fruit set and subsequent development.
(B) Molecular model for the regulation of feedback-regulated genes by SlDELLA and SlARF7/SlIAA9. Feedback-regulated genes involved in GA and auxin metabolism are repressed by the SlARF7/SlIAA9 complex but are induced by SlDELLA. Binding of SlDELLA to SlARF7 may sequester SlARF7 from the target gene promoters. SlDELLA may also recruit unidentified transcription factors (?) to activate transcription of these genes.
(C) Molecular model for the regulation of downstream fruit development-related genes by SlDELLA and SlARF7/SlIAA9. Fruit set and growth-related genes are repressed by the inhibition of SlARF7 activity by SlDELLA and SlIAA9 via direct protein-protein interactions. SlDELLA may also bind to unidentified transcription factor (?), which stabilizes SlARF7 binding to target promoters but inhibits its transactivation activity. Elevated levels of auxin and GA in fertilized ovule can trigger degradation of SlIAA9 and SlDELLA, respectively. This then allows SlARF7 (and additional activator SlARFs) to activate transcription of downstream growth-related genes.

possibility that auxin treatment of *gib1* ovaries was not effective, we generated *ARF7 RNAi gib1* (*ARF7i gib1*) and *entire gib1* (*e gib1*) homozygous double mutants by crosses to test whether enhanced auxin signaling by *ARF7 RNAi* or *entire* can promote parthenocarpy in *gib1*. Emasculation experiments showed no parthenocarpy in these double mutants compared with the *gib1* single mutant (Figures 7E and 7F). *e gib1* consistently produced smaller ovaries than *gib1* and *ARF7i gib1*, likely due to the pleiotropic effects of *entire*. Analysis of cross sections of the double mutant ovaries further confirmed that there was no difference in the number of cell layers or cell size compared with the *gib1* single mutant (Figures 7D and 7G). These results indicate that active GA biosynthesis is required for auxin to trigger fruit initiation and growth.

We also tested whether the expression of SlDELLA- and SlARF7/SlIAA9-target genes in *gib1* is responsive to GA and auxin treatment. As expected, both feedback- and growth-related downstream target genes in *gib1* responded to GA treatment in a manner similar to those in the wild type (Figure 7H). On the other hand, upon 2,4-D treatment, only the feedback-regulated genes were still responsive in *gib1*, while the expression of growth-related downstream genes was unaltered (Figure 7I). Therefore, under GA-deficiency conditions, auxin can still induce the expression of GA biosynthesis genes. However, in the absence of bioactive GA production, growth-related downstream target genes of SlDELLA/SlARF7/SlIAA9 are not responsive to auxin, as their expression is likely blocked by high levels of SlDELLA. To verify this idea, we tested whether SlDELLA protein levels are

Figure 7. (continued).

levels consistently increased 12 h after mock treatment, while GA application caused DELLA degradation in 1 h.
(L) 2,4-D and mock treatments of emasculated −1 DAA ovaries of *FLAG-DELLA pro gib1* did not affect DELLA levels over a 24-h period. By contrast, GA still caused the degradation of DELLA, as in *pro*.
In **(J)** to **(L)**, FLAG-DELLA was detected by immunoblot analysis with anti-FLAG antibody, and blots probed with α-tubulin were included to show equal loading.

affected by auxin in the wild-type *GIB1* and *gib1* mutant backgrounds. We used *FLAG-DELLA* transgenic lines, *FLAG-DELLA pro* and *FLAG-DELLA pro gib1*, for this analysis because FLAG-DELLA could readily be detected with an anti-FLAG antibody. As expected, FLAG-DELLA protein levels were much higher in *pro gib1* mutant than in *pro* due to the lack of bioactive GA in *gib1* (Figure 7J). For both *FLAG-DELLA* lines, emasculated –1 DAA ovaries were treated with 2,4-D or GA and harvested at different time points, and FLAG-DELLA levels were analyzed by immunoblot analysis. Figure 7K shows that under mock treatment, DELLA protein levels in the *FLAG-DELLA pro* line increased significantly at 12 h after emasculation and remained high at 24 h. There were no significant changes in the *DELLA* transcript levels at these time points (Supplemental Figure 7), indicating that the increased DELLA protein accumulation at 12 to 24 h is due to increased DELLA stability caused by the lack of GA production after emasculation. Under 2,4-D treatment, DELLA protein levels greatly decreased 12 h after emasculation and remained low at 24 h (Figure 7K), although its transcript levels remain unaltered (Supplemental Figure 7). In the *FLAG-DELLA pro gib1* line, FLAG-DELLA protein levels did not change after emasculation in the mock controls (Figure 7L), likely because FLAG-DELLA protein already accumulated to high levels in the *gib1* background due to GA deficiency. Importantly, auxin treatment did not reduce the levels of FLAG-DELLA accumulation in the *gib1* background (Figure 7L). GA treatment, which was used as a control, caused rapid degradation of FLAG-DELLA in both the *pro* and *pro gib1* backgrounds (Figures 7K and 7L). These results strongly suggest that auxin-induced tomato fruit initiation requires active GA biosynthesis and signaling to reduce the levels of the major repressor SlDELLA.

DISCUSSION

Our study revealed that SlDELLA and SlARF7/SlIAA9 mediate crosstalk between GA and auxin signaling pathways to regulate fruit initiation in tomato (Figure 8). SlDELLA induces the expression of GA biosynthesis genes (*GA20ox1* and *GA3ox1*) and *GH3.2* (encoding an auxin conjugating enzyme), which are known to be feedback-regulated genes by GA and auxin, respectively (Figure 8A). Coexpression of SlARF7 and SlIAA9, however, represses the expression of these feedback-regulated genes. Because SlARF7 and SlIAA9 directly interact, it is likely that the SlARF7/SlIAA9 complex functions as a transcriptional repressor to inhibit the transcription of these feedback-regulated genes (Figures 8A and 8B). Our data also indicate that SlDELLA directly interacts with SlARF7 and other activator SlARFs and that the coexpression of SlDELLA and SlARF7/SlIAA9 antagonistically regulates the feedback-regulated genes involved in GA biosynthesis and auxin deactivation (Figure 8A). ChIP-qPCR analysis indicated that both SlDELLA and SlARF7 associate with chromatin containing the promoters of these feedback-regulated genes. Reduced SlDELLA levels by GA treatment led to slightly increased SlARF7 binding to these feedback-regulated promoters. Therefore, the SlDELLA-SlARF7 interaction may sequester SlARF7 away from these target gene promoters. We also found that SlDELLA binds to the middle region of SlARF7 instead of its DNA binding domain, suggesting that the SlDELLA-SlARF7 interaction may alter the conformation of SlARF7. SlDELLA may also recruit unidentified DNA binding transcription factors to activate the transcription of these genes (Figure 8B); AtDELLAs activate the transcription of GA feedback-regulated genes through direct interactions with the zinc-finger transcription factors, INDETERMINATE DOMAIN family proteins (Fukazawa et al., 2014; Yoshida et al., 2014). A previous study (de Jong et al., 2011) also suggested that SlARF7 affects GA responses, as the morphology of parthenocarpic *SlARF7 RNAi* fruits was similar to that of GA-induced parthenocarpic fruits, and *GA20ox1* mRNA levels were higher in *SlARF7 RNAi* lines than in the wild type at anthesis. However, at 12 DAA, bioactive GA levels in the pericarps of parthenocarpic fruits of the *SlARF7 RNAi* lines were lower than those of wild-type fruits (de Jong et al., 2011). At this later stage, the high levels of GAs in wild-type pericarp could be due to the transport of GAs from developing seeds.

In contrast to the antagonistic effects of SlDELLA versus SlARF7/SlIAA9 on feedback-regulated genes, these proteins inhibit the expression of downstream growth-related genes (e.g., *EXP5*) and induce the expression of ethylene biosynthesis gene *ACO4* (Figure 8A), as shown by gene expression (Figures 6E and 6F) and ChIP-qPCR (Figure 5G) analyses. Previous studies have indicated that the activator ARFs function as transcriptional activators when they form ARF-ARF dimers (Ulmasov et al., 1999; Hardtke et al., 2004). We propose that before pollination, SlDELLA and SlIAA9 inhibit the expression of growth-related genes during fruit set by binding to SlARF7 (and other activator SlARFs) (Figure 8C). Interestingly, SlARF7 interacted with SlDELLA and SlIAA9 through distinct regions, and binding of SlDELLA or SlIAA9 did not affect the homodimerization of SlARF7 or its heterodimerization with other activator SlARFs. These results suggest that the binding of SlDELLA and SlIAA9 to activator SlARFs may directly inhibit their activity without interfering with their dimerization. Furthermore, our ChIP-qPCR data suggest that SlDELLA may enhance the binding of SlARF7 to downstream target promoters, whereas the association of SlDELLA with these targets is not affected by reduced levels of SlARFs in the *SlARF7 RNAi* line. One possibility is that SlDELLA also binds to other unidentified transcription factor(s), which stabilizes the binding of SlARF7 to target promoters but inhibits its transactivation activity (Figure 8C). Upon pollination, SlDELLA and SlIAA9 are degraded under elevated GA and auxin levels. This allows SlARF7 and other activator SlARFs to activate the transcription of the growth-related genes. Using the GA-deficient *gib1* mutant, we showed that auxin-induced tomato fruit initiation is GA dependent. In the *gib1* mutant background, elevated auxin signaling (via auxin treatment or *e* mutation) did not remove the high levels of SlDELLA protein. Based on this observation, one may consider that auxin functions upstream of the GA pathway. However, the additive effect of *e* (*iaa9*) and *pro* (*della*) indicates that both auxin and GA signals are necessary to remove both the auxin signaling repressor (IAA9) and GA signaling repressor (DELLA). Our biochemical and genetic studies provide support for the molecular interaction between GA and auxin pathways during fruit set. Our results help explain why both auxin and GA play important roles in fruit initiation and subsequent growth. Upon fertilization, auxin produced in the tomato ovule induces increased GA biosynthesis, which in turn triggers DELLA

degradation. At the same time, auxin induces the degradation of SlIAA9 (and possibly other SlIAAs), which is mediated by auxin receptors. Removing both key repressors (SlIAA and SlDELLA) releases SlARFs, allowing them to activate downstream genes that are important for fruit initiation and fruit growth.

The model presented in Figure 8 is supported by the observation that *pro* (*della*), *SlARF7 RNAi*, and *entire* (*iaa9*) have additive effects in promoting parthenocarpic fruit development, as shown by the phenotypes of the single and double mutants. In addition to SlARF7, it is likely that other activator SlARFs also play a role in controlling fruit set. We found that all activator SlARFs were expressed around anthesis, and they interacted with SlDELLA in Y2H assays. A recent study showed that amiRNA-induced downregulation of *SlARF5* expression resulted in parthenocarpy (Liu et al., 2018). We also showed that besides *SlARF7*, *SlARF5* and *SLARF8B* were downregulated in the *SlARF7 RNAi* line. Moreover, the *CR-slarf7 slarf5*/+ double mutant, but not its corresponding single mutants, produced parthenocarpic fruits, although at a lower frequency compared with the *ARF7 RNAi* line (Figures 2F and 6D). In addition, the average parthenocarpic fruit size of this double mutant was much smaller than that of the *ARF7 RNAi* line (Figure 2G). However, the *CR-slarf7 slarf5*/+ double mutant and the *ARF7 RNAi* line are in two different backgrounds (cultivar M82 versus MM), which may also contribute to the differences in their phenotypes. It is possible that *SlARF8B* also plays a role in fruit set, as this gene is expressed at quite high levels around anthesis and its expression is downregulated in the *SlARF7 RNAi* line. Taken together, our results support the idea that SlARF5, SlARF7, and additional SlARFs play overlapping roles in the regulation of fruit set. Based on the results of these genetic analyses, it is intriguing that these activator SlARFs appear to inhibit auxin-induced parthenocarpy. Considering that SlIAA9 represses auxin signaling by binding to activator ARFs, mutations in SlARF7 and SlARF5 may allow other activator SlARFs to induce downstream target genes more effectively if they have lower affinity to SlIAA9 than SlARF7 and SlARF5. Consistent with this idea, we found that SlARF8A and SlARF8B displayed weaker interactions with SlIAA9 than SlARF5 and SlARF7 in a Y2H assay (Figure 2A). As discussed above, our model also suggests that SlARF7 and other activator SlARFs promote fruit set when SlIAA9 and SlDELLA are degraded in response to elevated auxin and GA levels upon fertilization. The generation and characterization of single and multiple knockdown and knockout lines for additional activator SlARFs should help elucidate the specific and complex roles of individual SlARFs in fruit initiation.

Using the tomato system, we demonstrated that direct crosstalk between GA and auxin signaling pathways plays a role in controlling fruit initiation. Although recent studies in Arabidopsis reported an interaction between DELLA and ARF in Y2H and co-IP assays (Oh et al., 2014), the physiological effect of the DELLA-ARF interaction in planta is difficult to examine in Arabidopsis by genetic analysis, mainly due to the functional redundancy among the five AtDELLAs and the large numbers of AtARFs and AtIAAs. Importantly, the tomato genome contains only a single *SlDELLA* (*PRO*) gene. Although tomato contains many *IAA* genes, the single *entire* (*iaa9*) mutant displays a clear parthenocarpic phenotype. These unique features of the tomato system allowed us to elucidate the genetic interactions among SlDELLA, SlIAA9 and the activator SlARFs during fruit initiation.

METHODS

Plant Materials, Growth Conditions, and Statistical Analysis

Tomato (*Solanum lycopersicum*) cultivars AC and MM, and the *entire* mutant (in the AC background; Rick and Butler, 1956) were obtained from the Tomato Genetics Resource Center at UC Davis. The *pro* (5x bc AC; Smith and Ritchie, 1983) and *pro gib1* (Van Tuinen et al., 1999) mutants were gifts from Maarten Koornneef (Max Planck Institute for Plant Breeding Research, Germany), and the *ARF7 RNAi* line #4 (in the MM background) was generated by Wim Vriezen (de Jong et al., 2009). The AC/MM hybrid and double mutants *ARF7 RNAi pro*, *entire pro*, *entire ARF7 RNAi*, *ARF7 RNAi gib1*, and *entire gib1* were generated by genetic crosses. The *slarf5-1* (*slmp-1*, generated by EMS mutagenesis) and *CR-slarf7* mutants are in the M82 cultivar background. The *FLAG-DELLA pro gib1* line was produced by crossing the *FLAG-DELLA pro* transgenic line with *pro gib1*. Genotyping primers for the *pro*, *entire*, *gib1*, *CR-arf7*, and *arf5-1* mutants are listed in Supplemental Data Set 1.

Tomato plants were grown in the greenhouse with 16-h/8-h day/night light cycle. During the 16-h photoperiod, supplemental lights (Phillips 1000w Hortilux Super HPS) were turned on when internal light intensity was below 900 μmol/m^2/s for 30 min. Lights were turned off when internal light intensity exceeded 900 μmol/m^2/s for 30 min. Temperatures in the greenhouse were maintained at 21.1 to 26.7°C/18.3 to 23.9°C (day/night), and humidity was maintained between 37% and 72% RH. Flowers for emasculation and/or hormonal treatments were from the third to seventh flower trusses on the primary stem. For hormonal treatments, 10 μL of 300 μM GA_3, 100 μM 2,4-D, or mock solvent (5% methanol and 0.1% Tween 20) was applied to emasculated –1 DAA ovaries.

All statistical analyses were performed using Student's *t* test.

Plasmid Construction

Primers for plasmid construction are listed in Supplemental Data Set 1. PCR-generated DNA constructs were sequenced to make sure no mutation was introduced. Detailed information on plasmid construction is described in the Supplemental Data Set 2.

Y2H and Y3H Assays

The ProQuest Two-Hybrid system (Invitrogen) and yeast strain pJ69-4A were used for the Y2H and Y3H assays. Yeast transformation and 3-amino-1,2,4-triazole (3-AT) tests were performed as described previously (Dill et al., 2004) with slight modifications: 3-AT concentrations in the plates were 0, 5, 10, 25, 50, 75, and 100 mM in most cases, although concentrations of 150, 200, 250, and 300 mM 3-AT were used when the interactions were strong. Immunoblot analyses were performed using anti-HA (1:2000; Covance MMS-101P), anti-FLAG (1:5000; Sigma-Aldrich A8592), or anti-cMyc (1:2000; Covance MMS-150P) primary antibodies to show that the HA-DNA-BD, 3xFLAG-AD fusions in the Y2H assays and Myc-fusions in the Y3H assays produced the expected proteins in yeast.

Plant Transformation

Transformation of the $Pro_{SLDELLA}$*:FLAG-SlDELLA* construct into the *pro* mutant was performed by NCSU Plant Transformation Laboratory with *Agrobacterium tumefaciens* strain GV3101 pMP90. T0 lines containing a single insertion were identified by their T1 seeds having a 3:1 ratio of kanamycin-resistant versus kanamycin-sensitive segregation patterns.

All eight independent homozygous lines identified in the T1 generation rescued *pro* defects; line #C1-18-6 was chosen for further study.

Transient expression (for co-IP and the dual luciferase assays) in wild tobacco (*Nicotiana benthamiana*) leaves was performed as described (Zentella et al., 2016). Transient expression in tomato fruits (for ChIP) was performed based on a previous report (Orzaez et al., 2006), with slight modifications. Agrobacterium strain 1D1249 (a gift from Gregory Martin, Cornell University) containing the pEG203-ARF7 plasmid was used for this test. Incubation of 1D1249 cells in induction solution was performed as described for *N. benthamiana* infiltration (Zhang et al., 2011). The bacterial infiltration solution was injected into 2- to 3-cm-diameter wild-type fruits (2–3 weeks after anthesis) using a syringe with a 20-gauge needle; the needle was inserted into the stigma end of the fruit. When the needle was inserted halfway into the fruit, bacterial solution in the syringe was injected into the fruit until the solution emerged from the tips of sepals. Five days after infiltration, the jelly-like tissue in the fruit locules was harvested for ChIP-qPCR.

For the transient Myc-ARF7 expression +/–GA test, wild-type plants were drenched with 10 μM paclobutrazol three times a week for 2 weeks to increase DELLA levels in the fruit. One day before harvest (i.e., 4 d after infiltration), 300 μM GA_3 or mock solution was injected into Myc-ARF7 infiltrated fruits. Locular tissues were harvested on day 5 as described above. For transient Myc-DELLA ChIP, 1D1249 agrobacteria cells containing pEG203-DELLA plasmid were injected into wild-type or *ARF7 RNAi* fruits.

Quantitative RT-PCR

Total RNA was isolated using a Quick-RNA MiniPrep kit (Zymo Research). First-strand cDNA was synthesized using a Transcriptor First Strand cDNA Synthesis kit (Roche Applied Science). For qPCR, FastStart Essential DNA Green Master mix (Roche Applied Science) was used on a Mastercycler ep *realplex* Instrument (Eppendorf). The PCR program consisted of an initial denaturation at 95°C for 10 min, then 45 cycles of amplification at 95°C for 10 s, 60°C for 10 s, and 72°C for 15 s, followed by melting curve step at 95°C for 10 s, 65°C 60 s, and increases temperature at 0.1°C/s to 95°C for 1 s. Three biological replicates from independent pools of tissues (two technical repeats each) were included for each experiment. Primers for qPCR are listed in Supplemental Data Set 1.

For absolute qPCR analysis, the qPCR standard curves of *SlUBQ7* and *SlARF* genes were generated as described before (Tyler et al., 2004). For *SlUBQ7*, a 200-bp PCR product of *SlUBQ7* cDNA amplified by primers SlUBQ7-1 and SlUBQ7-2 from AC cDNAs was first inserted to pCR8/GW. Then, linearized pCR8-SlUBQ7 DNA was used as template for determining cDNA copy versus cycle number. For *SlARFs*, the DNA templates were linearized plasmids containing pCR8-*SlARF* cDNAs (except for *SlARF7*, which was in pENTR1A). Based on these standard curves, the cDNA copy numbers of *SlARF* genes and *SlUBQ7* were determined according to their respective cycle numbers.

Co-IP and Dual Luciferase Assay

Co-IP assays using proteins transiently expressed in *N. benthamiana* by agroinfiltration were performed as described previously (Zentella et al., 2016). The dual luciferase assays was also performed via transient expression in *N. benthamiana*. First reporter plasmids (*tomato gene promoter:fLUC* and Pro_{35S}*:rLUC*) and effector constructs (Pro_{35S}*:ARF7*, *DELLA*, or *IAA9* in pEarleyGate vector) were separately transformed into *Agrobacterium* strain GV3101. The *fLUC* and *rLUC*-containing strains were coinfiltrated into leaves, with various agro combinations of ARF7, DELLA, and IAA9 constructs. Two days after infiltration, *N. benthamiana* leaves were harvested for protein extraction, and luciferase activity was measured using the dual-luciferase reporter assay system (Promega). Relative promoter activity was calculated as the ratio of fLUC to rLUC activity for each sample. Nine biological repeats (three independent pools of tissue were assayed at one time and repeated at three different times) were conducted for each effector combination.

ChIP-qPCR

The ChIP-qPCR experiment was performed as described (Zentella et al., 2007), with slight modifications. For FLAG-SlDELLA ChIP, –1 DAA ovaries of the *FLAG-SlDELLA pro* transgenic tomato line were used. For transient SlARF7 ChIP, Myc-SlARF was transiently expressed in 2- to 3-cm-diameter wild-type fruits (2–3 weeks after anthesis) and the locule tissues were harvested and cross-linked for ChIP. Nontransgenic tissues (*pro* for SlDELLA ChIP and wild type + 1D1249 for SlARF7 ChIP) were included as controls. There were two modifications for the transient SlARF7 +/–GA ChIP. First, the wild-type plants were watered with 10 μM PAC for 2 weeks. Second, GA solution was injected into fruit 1 d before harvest. Nontransgenic tissues (wild type/PAC + 1D1249 –GA) were included as a control. For transient SlDELLA ChIP, Myc-SlDELLA was expressed in wild-type or *SlARF7 RNAi* fruit. 1D1249-infiltrated wild-type fruit was used as a control.

After cross-linking the tissues, chromatin was extracted as described by Zentella et al. (2007), and DNA was eluted from antibody-conjugated beads with modified elution buffer (20 mM Tris-HCl, pH 7.5, 5 mM EDTA, 50 mM NaCl, 1% SDS, and 50 μg/mL proteinase K). qRT-PCR was then performed using primers specific for different regions of the target promoters. The *SlUBQ7* gene (Solyc10g005560) was used to normalize the qPCR results in each ChIP sample. Primer sequences are listed in Supplemental Data Set 1.

Histology

After emasculation of flowers, ovaries were collected from *gib1*, *ARF7 RNAi gib1*, or *entire gib1* plants. Tissue fixation was performed as described (Hu et al., 2008), followed by tissue embedding in Technovit 7100 (Heraeus Kulzer) according to the manufacturer's protocol. Three-micrometer sections produced with a microtome (model 820; Spencer Lens Co.) were stained with 0.1% toluidine blue in 1% borax and examined by bright-field microscopy as described (Hu et al., 2008).

In Vitro IAA-Aspartic Acid Conjugation Assay

Recombinant GST, GST-SlGH3.2, and GST-AtGH3.6 were expressed in *Escherichia coli* BL21-CodonPlus (DE3)-RIL (Agilent Technologies). Induction and purification of recombinant proteins were performed as described by Zentella et al. (2016). The in vitro conjugation of IAA-aspartic acid and subsequent detection procedures basically followed a previous report (Staswick et al., 2005), with slight modifications. In particular, the conjugation reaction was performed at room temperature overnight in 50 μL solution containing 500 ng GST fusion proteins or GST. Six-microliter reactions were analyzed by thin-layer chromatography, and staining of IAA or IAA-Asp was done with Salkowski reagent.

Accession Numbers

Sequence information for genes included in this article can be found in the Sol Genomics Network and GenBank (for tomato genes) and TAIR network (https://www.arabidopsis.org/; for Arabidopsis genes) under the following accession numbers: *SlDELLA* (i.e., *PRO*, Solyc11g011260), *SlARF7* (Solyc07g042260), *SlIAA9* (i.e., *ENTIRE*, Solyc04g076850), *SlARF5* (Solyc04g084210), *SlARF8A* (Solyc03g031970), *SlARF8B* (Solyc02g037530), *SlARF19A* (Solyc07g016180; NM_001247811),

SlARF19B (Solyc05g047460; XM_010322983), *SlARF1* (Solyc01g103050), *SlARF2A* (Solyc03g118290), *SlARF2B* (Solyc12g042070), *SlARF3* (Solyc02g077560), *SlARF4* (Solyc11g069190), *SlARF9A* (Solyc08g082630), *SlARF10A* (Solyc11g069500), *SlARF16A* (Solyc09g007810), *SlARF24* (Solyc05g056040), *SlGA20ox1* (Solyc03g006880), *SlGA3ox1* (Solyc06g066820), *SlGH3.2* (Solyc01g107390), *SlAG1* (Solyc02g071730), *SlTM29* (Solyc02g089200), *JOINTLESS* (Solyc11g010570), *SlMADS6* (Solyc01g093960), *SlFUL1* (Solyc06g069430), *SlMADS29* (Solyc11g005120), *SlCYCB1;2* (Solyc10g080950), *SlEXP5* (Solyc02g088100), *SlEXP12* (Solyc05g007830), *SlXTH9* (Solyc12g011030), *SlXTH15* (Solyc03g031800), *SlABI2* (Solyc07g040990), *SlACO4* (Solyc02g081190), *SlERF1B* (Solyc09g066360), *SlCPS* (i.e., *GIB1*, Solyc06g084240), *SlUBQ7* (Solyc10g005560), *AtARF5* (At1g19850), *AtCPS* (At4g02780), and *AtGH3.6* (At5g54510).

Supplemental Data

Supplemental Figure 1. Activator SlARF hetero-dimerization is not affected by SlDELLA or SlIAA9 in a Y3H assay.

Supplemental Figure 2. Standard curves for absolute quantification of transcript levels by qPCR.

Supplemental Figure 3. GH3.2 functions as an amino acid-IAA conjugating enzyme in vitro.

Supplemental Figure 4. $Pro_{SlDELLA}$*:FLAG-DELLA* is functional in tomato.

Supplemental Figure 5. SlDELLA protein in fruit locule tissue accumulated to higher levels in response to PAC treatment and was completely degraded 24 h after GA_3 application.

Supplemental Figure 6. Response of putative GA/auxin target genes to GA or 2,4-D treatment in ovaries.

Supplemental Figure 7. *SlDELLA* transcript levels in emasculated –1 DAA ovaries compared with mock and hormone treatments.

Supplemental Data Set 1. List of primers and their uses.

Supplemental Data Set 2. Constructs.

ACKNOWLEDGMENTS

We thank Maarten Koornneef for providing *pro* and *procera gib1* mutants, Wim Vriezen and Ivo Rieu for the *SlARF7 RNAi* line, Miltos Tsiantis and Klaus Theres for providing pGPTV-Kan-PROCERA, Zachary B. Lippman for identifying the *slmp-1* mutation, and Yossi Capua and Yuval Eshed for providing the *SlARF7* construct. We also thank Gregory Martin for help with tomato transient expression, Neelima Sinha and Siobhan Brady for sharing protocols and tomato sequence information, George Allen and Sergei Krasnyanski at the Plant Transformation Laboratory at NC State University for tomato transformation, Rodolfo Zentella, Ning Sui, and Jonathan Dayan for generating the modified Y2H vectors, and Jiayu Chen for technical assistance. This work was supported by grants to T.-p.S. from the USDA (2010-65116-20460, 2014-67013-21548, and 2018-67013-27395), the National Institutes of Health (R01 GM100051), and the National Science Foundation (MCB-0923723).

AUTHOR CONTRIBUTIONS

J.H. and T.-p.S. designed the research. J.H. performed most experiments. N.O. identified the *slarf5-1* mutant. A.I. and N.O. generated the *CR-slarf7* single mutant and the *CR-slarf7 slarf5-1*/+ double mutant. J.H and T.-p.S. analyzed and wrote the manuscript.

Received May 7, 2018; revised June 21, 2018; accepted July 12, 2018; published July 15, 2018.

REFERENCES

Bensen, R.J., and Zeevaart, J.A. (1990). Comparison of *ent*-kaurene synthetase A and B activities in cell-free extracts from young tomato fruits of wild-type and *gib-1, gib-2*, and *gib-3* tomato plants. J. Plant Growth Regul. **9:** 237–242.

Boer, D.R., Freire-Rios, A., van den Berg, W.A., Saaki, T., Manfield, I.W., Kepinski, S., López-Vidrieo, I., Franco-Zorrilla, J.M., de Vries, S.C., Solano, R., Weijers, D., and Coll, M. (2014). Structural basis for DNA binding specificity by the auxin-dependent ARF transcription factors. Cell **156:** 577–589.

Brukhin, V., Hernould, M., Gonzalez, N., Chevalier, C., and Mouras, A. (2003). Flower development schedule in tomato *Lycopersicon esculentum* cv. sweet cherry. Sex. Plant Reprod. **15:** 311–320.

Carrera, E., Ruiz-Rivero, O., Peres, L.E., Atares, A., and Garcia-Martinez, J.L. (2012). Characterization of the procera tomato mutant shows novel functions of the SlDELLA protein in the control of flower morphology, cell division and expansion, and the auxin-signaling pathway during fruit-set and development. Plant Physiol. **160:** 1581–1596.

Chapman, E.J., and Estelle, M. (2009). Mechanism of auxin-regulated gene expression in plants. Annu. Rev. Genet. **43:** 265–285.

Davière, J.M., and Achard, P. (2016). A pivotal role of DELLAs in regulating multiple hormone signals. Mol. Plant **9:** 10–20.

de Jong, M., Wolters-Arts, M., Feron, R., Mariani, C., and Vriezen, W.H. (2009). The *Solanum lycopersicum* auxin response factor 7 (SlARF7) regulates auxin signaling during tomato fruit set and development. Plant J. **57:** 160–170.

de Jong, M., Wolters-Arts, M., García-Martínez, J.L., Mariani, C., and Vriezen, W.H. (2011). The *Solanum lycopersicum* AUXIN RESPONSE FACTOR 7 (SlARF7) mediates cross-talk between auxin and gibberellin signalling during tomato fruit set and development. J. Exp. Bot. **62:** 617–626.

Dharmasiri, N., Dharmasiri, S., and Estelle, M. (2005). The F-box protein TIR1 is an auxin receptor. Nature **435:** 441–445.

Dill, A., Thomas, S.G., Hu, J., Steber, C.M., and Sun, T.P. (2004). The Arabidopsis F-box protein SLEEPY1 targets gibberellin signaling repressors for gibberellin-induced degradation. Plant Cell **16:** 1392–1405.

Dorcey, E., Urbez, C., Blázquez, M.A., Carbonell, J., and Perez-Amador, M.A. (2009). Fertilization-dependent auxin response in ovules triggers fruit development through the modulation of gibberellin metabolism in Arabidopsis. Plant J. **58:** 318–332.

Du, L., Bao, C., Hu, T., Zhu, Q., Hu, H., He, Q., and Mao, W. (2016). SmARF8, a transcription factor involved in parthenocarpy in eggplant. Mol. Genet. Genomics **291:** 93–105.

Fuentes, S., Ljung, K., Sorefan, K., Alvey, E., Harberd, N.P., and Østergaard, L. (2012). Fruit growth in Arabidopsis occurs via DELLA-dependent and DELLA-independent gibberellin responses. Plant Cell **24:** 3982–3996.

Fukazawa, J., Teramura, H., Murakoshi, S., Nasuno, K., Nishida, N., Ito, T., Yoshida, M., Kamiya, Y., Yamaguchi, S., and Takahashi, Y. (2014). DELLAs function as coactivators of GAI-ASSOCIATED FACTOR1 in regulation of gibberellin homeostasis and signaling in Arabidopsis. Plant Cell **26:** 2920–2938.

Gillaspy, G., Ben-David, H., and Gruissem, W. (1993). Fruits: A developmental perspective. Plant Cell **5:** 1439–1451.

Goetz, M., Vivian-Smith, A., Johnson, S.D., and Koltunow, A.M. (2006). AUXIN RESPONSE FACTOR8 is a negative regulator of fruit initiation in Arabidopsis. Plant Cell **18:** 1873–1886.

Gorguet, B., van Heusden, A.W., and Lindhout, P. (2005). Parthenocarpic fruit development in tomato. Plant Biol (Stuttg) **7:** 131–139.

Guilfoyle, T.J. (2015). The PB1 domain in auxin response factor and Aux/IAA proteins: a versatile protein interaction module in the auxin response. Plant Cell **27:** 33–43.

Guilfoyle, T.J., and Hagen, G. (2007). Auxin response factors. Curr. Opin. Plant Biol. **10:** 453–460.

Hardtke, C.S., Ckurshumova, W., Vidaurre, D.P., Singh, S.A., Stamatiou, G., Tiwari, S.B., Hagen, G., Guilfoyle, T.J., and Berleth, T. (2004). Overlapping and non-redundant functions of the Arabidopsis auxin response factors MONOPTEROS and NONPHOTOTROPIC HYPOCOTYL 4. Development **131:** 1089–1100.

Hu, J., et al. (2008). Potential sites of bioactive gibberellin production during reproductive growth in Arabidopsis. Plant Cell **20:** 320–336.

Kepinski, S., and Leyser, O. (2005). The Arabidopsis F-box protein TIR1 is an auxin receptor. Nature **435:** 446–451.

Koornneef, M., Bosma, T.D., Hanhart, C.J., van der Veen, J.H., and Zeevaart, J.A. (1990). The isolation and characterization of gibberellin-deficient mutants in tomato. Theor. Appl. Genet. **80:** 852–857.

Kumar, R., Agarwal, P., Tyagi, A.K., and Sharma, A.K. (2012). Genome-wide investigation and expression analysis suggest diverse roles of auxin-responsive GH3 genes during development and response to different stimuli in tomato (*Solanum lycopersicum*). Mol. Genet. Genomics **287:** 221–235.

Liu, S., Zhang, Y., Feng, Q., Qin, L., Pan, C., Lamin-Samu, A.T., and Lu, G. (2018). Tomato AUXIN RESPONSE FACTOR 5 regulates fruit set and development via the mediation of auxin and gibberellin signaling. Sci. Rep. **8:** 2971.

Livne, S., Lor, V.S., Nir, I., Eliaz, N., Aharoni, A., Olszewski, N.E., Eshed, Y., and Weiss, D. (2015). Uncovering DELLA-independent gibberellin responses by characterizing new tomato procera mutants. Plant Cell **27:** 1579–1594.

Martí, C., Orzáez, D., Ellul, P., Moreno, V., Carbonell, J., and Granell, A. (2007). Silencing of DELLA induces facultative parthenocarpy in tomato fruits. Plant J. **52:** 865–876.

McGinnis, K.M., Thomas, S.G., Soule, J.D., Strader, L.C., Zale, J.M., Sun, T.P., and Steber, C.M. (2003). The Arabidopsis *SLEEPY1* gene encodes a putative F-box subunit of an SCF E3 ubiquitin ligase. Plant Cell **15:** 1120–1130.

Mignolli, F., Vidoz, M.L., Mariotti, L., Lombardi, L., and Picciarelli, P. (2015). Induction of gibberellin 20-oxidases and repression of gibberellin 2 beta-oxidases in unfertilized ovaries of entire tomato mutant, leads to accumulation of active gibberellins and parthenocarpic fruit formation. Plant Growth Regul. **75:** 415–425.

Mockaitis, K., and Estelle, M. (2008). Auxin receptors and plant development: a new signaling paradigm. Annu. Rev. Cell Dev. Biol. **24:** 55–80.

Murase, K., Hirano, Y., Sun, T.P., and Hakoshima, T. (2008). Gibberellin-induced DELLA recognition by the gibberellin receptor GID1. Nature **456:** 459–463.

Oh, E., Zhu, J.Y., Bai, M.Y., Arenhart, R.A., Sun, Y., and Wang, Z.Y. (2014). Cell elongation is regulated through a central circuit of interacting transcription factors in the Arabidopsis hypocotyl. eLife **3:** 03031.

Orzaez, D., Mirabel, S., Wieland, W.H., and Granell, A. (2006). Agroinjection of tomato fruits. A tool for rapid functional analysis of transgenes directly in fruit. Plant Physiol. **140:** 3–11.

Ozga, J.A., Reinecke, D.M., Ayele, B.T., Ngo, P., Nadeau, C., and Wickramarathna, A.D. (2009). Developmental and hormonal regulation of gibberellin biosynthesis and catabolism in pea fruit. Plant Physiol. **150:** 448–462.

Park, J.E., Park, J.Y., Kim, Y.S., Staswick, P.E., Jeon, J., Yun, J., Kim, S.Y., Kim, J., Lee, Y.H., and Park, C.M. (2007). GH3-mediated auxin homeostasis links growth regulation with stress adaptation response in Arabidopsis. J. Biol. Chem. **282:** 10036–10046.

Peng, J., Carol, P., Richards, D.E., King, K.E., Cowling, R.J., Murphy, G.P., and Harberd, N.P. (1997). The Arabidopsis *GAI* gene defines a signaling pathway that negatively regulates gibberellin responses. Genes Dev. **11:** 3194–3205.

Rick, C.M., and Butler, L. (1956). Cytogenetics of tomato. Adv. Genet. **7:** 267–382.

Ruan, Y.L., Patrick, J.W., Bouzayen, M., Osorio, S., and Fernie, A.R. (2012). Molecular regulation of seed and fruit set. Trends Plant Sci. **17:** 656–665.

Salehin, M., Bagchi, R., and Estelle, M. (2015). SCFTIR1/AFB-based auxin perception: mechanism and role in plant growth and development. Plant Cell **27:** 9–19.

Serrani, J.C., Fos, M., Atares, A., and Garcia-Martinez, J.L. (2007). Effect of gibberellin and auxin on parthenocarpic fruit growth induction in the cv Micro-Tom of tomato. J. Plant Growth Regul. **26:** 211–221.

Serrani, J.C., Ruiz-Rivero, O., Fos, M., and García-Martínez, J.L. (2008). Auxin-induced fruit-set in tomato is mediated in part by gibberellins. Plant J. **56:** 922–934.

Seymour, G.B., Østergaard, L., Chapman, N.H., Knapp, S., and Martin, C. (2013). Fruit development and ripening. Annu. Rev. Plant Biol. **64:** 219–241.

Shinozaki, Y., et al. (2015). Ethylene suppresses tomato (*Solanum lycopersicum*) fruit set through modification of gibberellin metabolism. Plant J. **83:** 237–251.

Silverstone, A.L., Ciampaglio, C.N., and Sun, T. (1998). The Arabidopsis RGA gene encodes a transcriptional regulator repressing the gibberellin signal transduction pathway. Plant Cell **10:** 155–169.

Smith, J.W., and Ritchie, D.B. (1983). A collection of near-isogenic lines tomato: research tool of the future? Plant Mol. Biol. Report. **1:** 41–45.

Srivastava, A., and Handa, A.K. (2005). Hormonal regulation of tomato fruit development: a molecular perspective. J. Plant Growth Regul. **24:** 67–82.

Staswick, P.E., Tiryaki, I., and Rowe, M.L. (2002). Jasmonate response locus JAR1 and several related Arabidopsis genes encode enzymes of the firefly luciferase superfamily that show activity on jasmonic, salicylic, and indole-3-acetic acids in an assay for adenylation. Plant Cell **14:** 1405–1415.

Staswick, P.E., Serban, B., Rowe, M., Tiryaki, I., Maldonado, M.T., Maldonado, M.C., and Suza, W. (2005). Characterization of an Arabidopsis enzyme family that conjugates amino acids to indole-3-acetic acid. Plant Cell **17:** 616–627.

Sun, T.P. (2010). Gibberellin-GID1-DELLA: a pivotal regulatory module for plant growth and development. Plant Physiol. **154:** 567–570.

Tang, N., Deng, W., Hu, G., Hu, N., and Li, Z. (2015). Transcriptome profiling reveals the regulatory mechanism underlying pollination dependent and parthenocarpic fruit set mainly mediated by auxin and gibberellin. PLoS One **10:** e0125355.

Tyler, L., Thomas, S.G., Hu, J., Dill, A., Alonso, J.M., Ecker, J.R., and Sun, T.P. (2004). Della proteins and gibberellin-regulated seed germination and floral development in Arabidopsis. Plant Physiol. **135:** 1008–1019.

Ueguchi-Tanaka, M., Ashikari, M., Nakajima, M., Itoh, H., Katoh, E., Kobayashi, M., Chow, T.Y., Hsing, Y.I., Kitano, H., Yamaguchi, I., and Matsuoka, M. (2005). GIBBERELLIN INSENSITIVE DWARF1 encodes a soluble receptor for gibberellin. Nature **437:** 693–698.

Ulmasov, T., Hagen, G., and Guilfoyle, T.J. (1999). Dimerization and DNA binding of auxin response factors. Plant J. **19:** 309–319.

Van Tuinen, A., Peters, A.H.L.J., Kendrick, R.E., Zeevaart, J.A.D., and Koornneef, M. (1999). Characterisation of the *procera* mutant of tomato and the interaction of gibberellins with end-of-day far-red light treatments. Physiol. Plant. **106:** 121–128.

Vernoux, T., et al. (2011). The auxin signalling network translates dynamic input into robust patterning at the shoot apex. Mol. Syst. Biol. **7:** 508.

Vriezen, W.H., Feron, R., Maretto, F., Keijman, J., and Mariani, C. (2008). Changes in tomato ovary transcriptome demonstrate complex hormonal regulation of fruit set. New Phytol. **177:** 60–76.

Wang, H., Jones, B., Li, Z., Frasse, P., Delalande, C., Regad, F., Chaabouni, S., Latché, A., Pech, J.C., and Bouzayen, M. (2005). The tomato Aux/IAA transcription factor IAA9 is involved in fruit development and leaf morphogenesis. Plant Cell **17:** 2676–2692.

Yoshida, H., et al. (2014). DELLA protein functions as a transcriptional activator through the DNA binding of the indeterminate domain family proteins. Proc. Natl. Acad. Sci. USA **111:** 7861–7866.

Zentella, R., et al. (2016). O-GlcNAcylation of master growth repressor DELLA by SECRET AGENT modulates multiple signaling pathways in Arabidopsis. Genes Dev. **30:** 164–176.

Zentella, R., Zhang, Z.L., Park, M., Thomas, S.G., Endo, A., Murase, K., Fleet, C.M., Jikumaru, Y., Nambara, E., Kamiya, Y., and Sun, T.P. (2007). Global analysis of della direct targets in early gibberellin signaling in Arabidopsis. Plant Cell **19:** 3037–3057.

Zhang, J., Chen, R., Xiao, J., Qian, C., Wang, T., Li, H., Ouyang, B., and Ye, Z. (2007). A single-base deletion mutation in SlIAA9 gene causes tomato (*Solanum lycopersicum*) entire mutant. J. Plant Res. **120:** 671–678.

Zhang, Z.L., Ogawa, M., Fleet, C.M., Zentella, R., Hu, J., Heo, J.O., Lim, J., Kamiya, Y., Yamaguchi, S., and Sun, T.P. (2011). Scarecrow-like 3 promotes gibberellin signaling by antagonizing master growth repressor DELLA in Arabidopsis. Proc. Natl. Acad. Sci. USA **108:** 2160–2165.

Zouine, M., Fu, Y., Chateigner-Boutin, A.L., Mila, I., Frasse, P., Wang, H., Audran, C., Roustan, J.P., and Bouzayen, M. (2014). Characterization of the tomato ARF gene family uncovers a multi-levels post-transcriptional regulation including alternative splicing. PLoS One **9:** e84203.